VTT Technical Research Centre of Finland

Identification and metabolism of naturally prevailing microorganisms in zinc and copper mineral processing

Miettinen, Hanna; Bomberg, Malin; Le, Thi Minh Khanh; Kinnunen, Päivi

Published in:
Minerals

DOI:
10.3390/min11020156

Published: 02/02/2021

Document Version
Publisher's final version

minerals

MDPI

Article

Identification and Metabolism of Naturally Prevailing Microorganisms in Zinc and Copper Mineral Processing

Hanna Miettinen [1,*], Malin Bomberg [1], Thi Minh Khanh Le [2] and Päivi Kinnunen [3]

[1] VTT Technical Research Centre of Finland Ltd., Tietotie 2, FIN-02150 Espoo, Finland; malin.bomberg@vtt.fi
[2] Department of Bioproducts and Biosystems, School of Chemical Engineering, Aalto University, P.O. Box 16300, 00076 Aalto, Finland; thi.5.le@aalto.fi
[3] VTT Technical Research Centre of Finland Ltd., Visiokatu 4, P.O. Box 1300, 33101 Tampere, Finland; paivi.kinnunen@vtt.fi
* Correspondence: hanna.miettinen@vtt.fi; Tel.: +358-40-571-8267

Abstract: It has only recently been discovered that naturally prevailing microorganisms have a notable role in flotation in addition to chemical process parameters and overall water quality. This study's aim was to assess the prevailing microbial communities in relation to process chemistry in a zinc and copper mineral flotation plant. Due to the limitations of cultivation-based microbial methods that detect only a fraction of the total microbial diversity, DNA-based methods were utilised. However, it was discovered that the DNA extraction methods need to be improved for these environments with high mineral particle content. Microbial communities and metabolism were studied with quantitative PCR and amplicon sequencing of bacterial, archaeal and fungal marker genes and shotgun sequencing. Bacteria dominated the microbial communities, but in addition, both archaea and fungi were present. The predominant bacterial metabolism included versatile sulfur compound oxidation. Putative *Thiovirga* sp. dominated in the zinc plant and the water circuit samples, whereas *Thiobacillus* spp. dominated the copper plant. *Halothiobacillus* spp. were also an apparent part of the community in all samples. Nitrogen metabolism was more related to assimilatory than dissimilatory nitrate and nitrite oxidation/reduction reactions. Abundance of heavy metal resistance genes emphasized the adaptation and competitive edge of the core microbiome in these extreme conditions compared to microorganisms freshly entering the process.

Keywords: bacteria; archaea; fungi; flotation; sulfur; heavy metal resistance; core microbiome; water quality; DNA

Citation: Miettinen, H.; Bomberg, M.; Le, T.M.K.; Kinnunen, P. Identification and Metabolism of Naturally Prevailing Microorganisms in Zinc and Copper Mineral Processing. *Minerals* **2021**, *11*, 156. https://doi.org/10.3390/min11020156

Academic Editor: Sabrina Hedrich
Received: 2 December 2020
Accepted: 27 January 2021
Published: 2 February 2021

1. Introduction

Metal mining is facing limited availability of commodities, such as energy and water. This is forcing the mining sector to optimize and consider all available alternatives to ensure economic, efficient, safe and environmentally friendly plant performance. Issues such as energy consumption, water use/recycling and water quality, along with the utilization of low-grade ores, comprise the major challenges [1,2]. Traditionally, these challenges have been met with physico-chemical approaches. In recent decades, bio-based technologies have offered some environmentally benign approaches, such as bioleaching, bioflotation/flocculation and bioremediation (reviewed by [3,4]). Many of these bio-based approaches have been used only in limited amounts of often specialised applications [1] and they still await being exploited at their full scale and potential. Nevertheless, microorganisms, in addition to abiotic chemical and physical factors, have been said to play significant roles in flotation both in laboratory and at full scale [5–7].

Active microorganisms can be found in all habitats on Earth that provide at least low amounts of basic nutrients for growth and maintenance of metabolic functions [8]. The types and amounts of required nutrients vary depending on the microorganism in question, or vice versa—microorganisms present depend on the environment they are

adapted to. In principle, all environments are habitable, as microorganisms can adapt to extreme conditions, such as temperatures between −20 and 122 °C, pressures up to 110 MPa and extremely acidic pH 0 to alkaline pH 12.8 conditions [9]; and they survive even in more demanding conditions for short periods. Thus, it is reasonable to expect that mineral processing environments other than bioleaching processes also harbor notable amounts of microorganisms, which was recently verified [10]. These naturally occurring microorganisms may pass through the process without really affecting it. Nevertheless, there likely are microorganisms that are adapted to different parts and conditions within stages of mineral processing [11] where they are able to multiply and form biofilms. The role of these still unexplored naturally prevailing microbial communities is largely unknown in mineral processing, but already there is some indication of their effect on flotation performance, especially in connection with increased water recycling [7]. Water recirculation is likely to increase the water temperatures due to the shorter water circuits and accumulations of various chemical compounds [12]. Both of these stimulate microbial activity, proliferation and accumulation.

Microorganisms affect their surroundings by performing redox reactions, and producing proteins, extracellular polysaccharides and biosurfactants. Some of these compounds and the cell itself may function as flocculants, depressants, biocollectors or biofrothers in flotation (reviewed in [5]). However, microorganisms are also particles with mostly negatively charged surfaces [13]. This surface charge is pH dependent, and above the isoelectric point of the whole cell the net charge is negative. Some bacterial strains have an isoelectric point as high as pH 11 [13]. In flotation, mineral particles are separated based on their hydrophobicity differences affected by chemical compounds into gas, liquid and solid phases, making it a complicated, dynamic process. The presence of high numbers of microbial cells of different species and different activities and surface characteristics complicates the system further. Overall, the behavior and the effects of microorganisms in flotation depend most likely distinctly on the features of each microorganism type and the process step. This in turn is affected by parameters such as flotation reagents, pH, temperature and other water quality variables, including energy sources for microorganisms. Due to the complexity of interactions, the system should be studied in situ to best identify the factors affecting microbial and physicochemical behavior in the actual environment. For this reason, it is important to obtain knowledge of the microbial groups, their abundances and their metabolisms present in different parts of operating mineral processing plants.

It is generally acknowledged that only a fraction of the microorganisms found in the environment are able to grow on different growth media in the laboratory [14], and that the culturable community is greatly biased towards taxa that thrive in the culture's conditions [10]. Traditional cultivation also demands the use of a multitude of media and conditions to cover different microbial needs. The sparse microbiological studies focusing on mineral processing plants [7,11] have relied on cultivation-based techniques, and to our knowledge, no direct DNA extraction method has been applied, except very recently [10,15]. Cultivation-independent methods based on DNA-extraction are more likely to discover diverse microbial communities. However, successful DNA extraction from different sample types is needed.

Our study is one of the first to widely characterize and assess the prevailing microbial communities in different parts of a mineral processing plant. The novelty of this study is based on extensive microbiological data from multiple process steps supported by water quality data from two mineral processing plants. We studied the diversity, abundance and potential metabolisms of bacterial, archeal and fungal communities in relation to chemical parameters in the flotation processes of zinc and copper plants and adjacent water circuits. This study serves as a base for more extensive future research into specific microbe-related phenomena occurring in mineral processing and describes the microbial conditions in this environment in general. There is still very limited knowledge about how the microbial components in this environment react to changes in the process (e.g., ore quality, flotation reagents, temperature) and whether the microorganisms affect the processing conditions.

Sampling was performed in Portugal during summer (June) and winter (November) seasons in 2018 in order to identify seasonal effects. Bacteria predominated the mineral processing microbiomes, with abundant metabolism related to reduced sulfur compound oxidation. This study is part of the H2020 ITERAMS project (grant agreement# 730480), which strives to improve the recycling of water and minimize the environmental impact of mines.

2. Materials and Methods

2.1. Sampling Site

The mine site is situated in Portugal. The mineral deposits of the Iberian Pyrite are classified as volcano-sedimentary massive sulfide. They occur typically as lenses of polymetallic, copper, zinc, tin and lead, massive sulfides. The underground mine produces ore for the processing facility comprising of copper and zinc plants. The plants produce zinc, lead (Figure 1A) and copper concentrates (Figure 1B). Flotation chemicals used in the zinc plant are sodium metabisulfite (MBS), mineral collector 527E, which is an aqueous solution of dialkyl dithiophosphate and thiocarbamate, promoter/collector 3418A a sodium diisobutyldithiophosphinate, activator $CuSO_4$ and sodium isobutyl xanthate SIBX, which is an anionic collector. In the copper plant, the used reagents are the same without the collector 3418A and in addition lime is used.

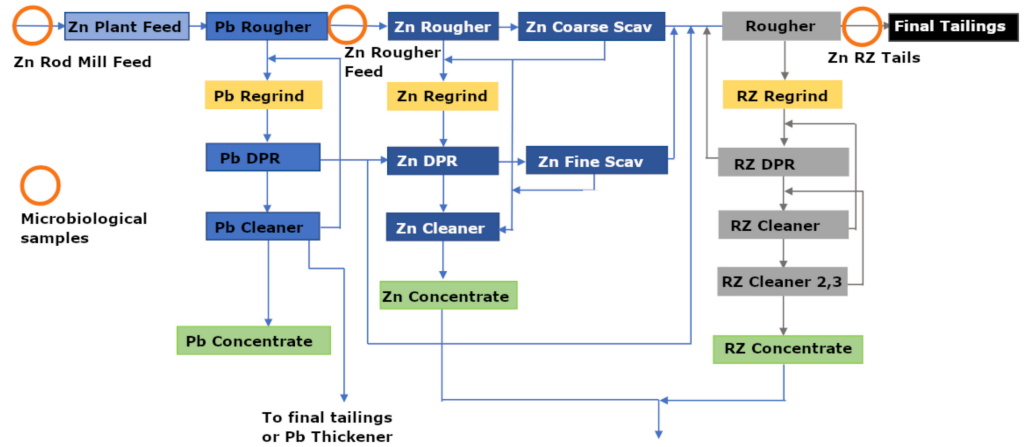

Figure 1. A schematic simplified representation of the zinc (**A**) and copper (**B**) process plants and microbial sampling points (orange circles). Additionally, microbial samples were taken from mine water treatment plant (ETAM) In and Out flows, Paste Thickener Overflow and the raw water source Santa Clara reservoir.

The tailings from the processing plants are transfered to the paste plant. The paste plant, which is a series of two paste thickeners, thickens the tailings for disposal in the paste cell and discharges most of the paste thickener overflow to the industrial water tanks (TAI). In the case of excess, the mine clarifier overflow is pumped to the water treatment plant (ETAM), where it is treated with the tailings ponds run-off water and used in the process plant as gland seal water.

2.2. Samples

Water samples were collected on two occasions in 2018 on 5–7 June and 20–22 November, in order to detect possible seasonal changes in the microbial communities. The air temperature during the June sampling campaign ranged from 13 to 22 °C and during the November sampling between 4 and 17 °C. The weather was dry at all times. The twelve sampling points with their chemical characteristics are presented in the Table 1 and Figures 2–4. Rod Mill Feed, Rougher Feed and Final Tailings were sampled from both copper and zinc plants. In addition, Copper Concentrate Thickener Overflow and Industrial Water (TAI) were studied from the copper plant. The water circuit was studied from four points—i.e., the Santa Clara water reservoir used to supplement water need; the Mine Water Treatment Plant (ETAM) from In and Out flows; and finally, the Paste Thickener Overflow.

Samples were collected on site into 5 L clean plastic buckets by the mine personnel and within two hours filtered in triplicate on 0.22 µm pore-size SterivexTM polyethersulfone (PES) filters (Merck, Burlington, MA, USA) using a peristaltic pump equipped with sterile silicon tubing while continuously mixing the water with a sterile spoon. The filtered sample size ranged from 250 mL to 720 mL depending on the particulate amount clogging the filter in each sample. The differences in the triplicate sample sizes were all within 50 mL and the volumes were generally the same for all replicates. Only the copper plant Rougher Feed June sample was an exception as its total volume was so small that it resulted as only one liquid sample, a mixture of liquid and sediment and a sediment sample. After filtering the samples, the filters were placed in sterile 50 mL plastic test tubes equipped with screw caps and frozen at −20 °C. A few additional samples were also frozen at −20 °C in glycerol (final glycerol concentration 10 % v/v) at the sampling site in sterile 15 mL plastic tubes for microscopy. The frozen samples were shipped in a cooling box with dry ice to Espoo, Southern Finland. The samples remained frozen over the transportation period and were kept at −20 °C until DNA extraction or microscopy.

2.3. Microscopy

Samples stored frozen in glycerol were thawed, 30 µL aliquots of the mixed sample were stained with 10 µL of 4′,6-dioamidino-2-phenylindole (DAPI, Sigma-Aldrich D9542, Merck) stain (0.5 mg mL^{-1} in 0.9% NaCl). After 15 min incubation in the dark, samples were spread on microscopy slides and examined using an Axio Imager M2 epifluorescence microscope with 100x magnification (Carl Zeiss Microscopy, Göttingen, Germany) equipped with a digital camera (AxioCam MRm, Carl Zeiss Microscopy). The images were acquired and analysed using the Zen 2.3 (blue edition) software (Carl Zeiss Microscopy).

2.4. DNA Extraction

DNA was extracted using the NucleoSpin Soil DNA extraction kit (Macherey-Nagel GmbH and Co, KG, Düren, Germany) with using the lysis buffer SL1 in combination with the enhancer solution SX according to the manufacturer's instructions. The Sterivex filter units were thawed on ice and placed in sterile plastic bags, and carefully smashed open with a hammer. The plastic bags were carefully opened in a laminar flow hood avoiding contamination, and the filters were cut from the central cylinder of the filtration unit using sterile scalpels and placed in sterile 5 mL centrifugation tubes containing the beads from one bead tube of the DNA extraction kit together with twfold reagent amounts. In order to release the microorganisms from the filters the tubes were vortexed for 5 min horizontally

with the lysis buffer. The tubes were centrifuged in an Eppendorf 5810R benchtop at 3184× *g* for 5 min, after which the supernatant continued in the DNA extraction according to the manufacturer's protocol. The DNA was eluted in 100 µL elution buffer SE. The DNA extracts were further purified using the NucleoSpin gDNA Clean-up kit (Macherey-Nagel) according to the manufacturer's protocol. The DNA was eluted in the original volume. The concentration of extracted DNA was measured with the Qubit 2.0 Fluorometer (Fisher Scientific, Loughborough, UK) according to the manufacturer's instructions.

2.5. Estimation of Community Size

Quantitative PCR (qPCR) of the bacterial and archaeal 16S rRNA genes and the fungal 5.8S rRNA genes was used as a proxy to estimate the microbial community sizes. The size of the bacterial communities was estimated using primers S-D-Bact-0341-b-S-17/S-D-Bact-0785-a-A-21 [16], producing a 400-bp fragment covering the variable region V3-V4 of the bacterial 16S rRNA gene. The qPCR reactions were performed using the SensiFAST Sybr No-ROX kit (Bioline, Meridian Biosciences, Cincinnati, OH, USA). The reactions contained 800 nM of each primer, and 1 µL template DNA in white 96-well plates with transparent film cover (4titude, Brooks Life Sciences, Chelmsford, MA, USA). The amplification programme consisted of an initial denaturation step at 95 °C for 15 min, followed by 40 amplification cycles of 10 s at 95 °C, 35 s at 57 °C and 30 s at 72 °C; and a final elongation step of 3 min at 72 °C and melting curve analysis.

The archaeal community size was tested with primers A344F [17] and A744R, modified from Barns et al. [18] flanking an approximately a 400-bp fragment containing the V3-V4 regions of the archaeal 16S rRNA gene according to the method described in [19]. The amplification was detected with a FAM-labeled probe, A516F [20] using the SensiFAST Probe No-ROX kit. The fungal community sizes were estimated using the fungal 5.8S rRNA gene as target. The fungal 5.8S rRNA gene fragment was amplified with primers 5.8F1 and 5.8R1 and detected with a FAM-labeled probe 5.8P1 according to Haugland et al. [21] using the SensiFAST Probe No-ROX kit. Both the archaeal and fungal reactions contained 500 nM of each primer and 200 nM probe. Both the amplification reaction consisted of enzyme activation at 95 °C for 3 min and 40 cycles of 10 s at 95 °C, 30 s at 62 °C and 1 s at 72 °C.

All the bacterial, archaeal and fungal amplifications were performed in triplicate using 10 µL reaction volumes and 1 µL of template DNA and run on the LightCycler 480 instrument. Negative controls without added DNA template were included in each run. The bacterial, archaeal and fungal amplification results were compared to that of a plasmid standard dilution series containing the 16S rRNA gene insert of *Escherichia coli* or *Halobacterium salinarum*, for bacteria and archaea, respectively, or the 5.8S rRNA gene of *Aspergillus versicolor* for fungi.

2.6. Amplicon Sequencing and Sequence Analysis

The bacterial amplicon libraries were produced with primers Bact_0341F/Bact_805R [16], flanking the variable region V3-V4 of the 16S rRNA gene and archaeal amplicon libraries with primers S-D-Arch-0349-a-S-17/S-D-Arch-0787-a-A-20 [22] targeting the V3-V4 region of the 16S rRNA gene. The fungal communities were characterized using the internal transcribed spacer gene marker region 1 (ITS1) and amplicon libraries were produced with primer pair ITS1 and ITS2 [23,24]. The ITS1 region was selected for the amplicon sequencing due to more extensive ITS database availability compared to databases for the 5.8S rRNA gene, whereas the 5.8S rRNA gene is more applicable for the probe-based qPCR analysis, as the 5.8S rRNA gene contains conserved regions for the probe to bind to. Parallel 25 µL amplification reactions were prepared for each sample in 2x MyTaq™ Red Mix (Bioline), with 800 nM of each primer, filled up to 25 µL molecular-biology-grade water and 2 µL of template. The PCR program contained an initial denaturation step at 95 °C for 3 min, followed by 35 cycles for bacteria and fungi and 40 cycles for archaea of 15 s denaturation at 95 °C, 15 s primer annealing at 50 °C, and 15 s elongation at 72 °C, and a final 30 s elongation step at 72 °C. The PCR products were verified with agarose gel

electrophoresis before they were sent for sequencing on the Ion Torrent PGM platform at Bioser (Biocenter Oulu Sequencing Center, Oulu, Finland). The amplicons were further purified and size-selected before sequencing by the staff at Bioser. For samples, from which only few bacterial 16S rRNA gene sequence reads were obtained, new amplicon libraries were prepared and sequenced.

The sequence reads were analyzed using the Mothur software (v.1.43.0) [25] to remove adapter, barcode and primer sequences, and to exclude sequences that did not meet the quality criteria (no barcode mismatches, maximum two primer mismatches, no ambiguous nucleotides, maximum eight nucleotide long homopolymer stretches and minimum length of 250 bp for bacteria and archaea and 200 bp for fungal ITS sequences). A qwindowaverage of 25 and a qwindowsize of 50 were used on the PGM read data in order to remove erroneous reads from the data set.

The Silva database version 138 [26,27] was optimized to cover the same region as the amplicons using the pcr.seqs command in mothur separately for bacteria and archaea. The bacterial and archaeal 16S rRNA sequences were aligned with Mothur to the optimized Silva reference alignment. Chimeric sequence reads were removed with vsearch in Mothur, where after the dereplicated sequences were classified using the optimized Silva reference alignment and taxonomy database using a cutoff of 80. Sequences that were not classified as bacteria were removed from the bacterial sequence data, and sequences failing to be classified as archaea were removed from the archaeal sequence data. A distance matrix was calculated using the dist.seqs command in Mothur with default parameters. The filtered sequences were clustered in to OTUs (Operational Taxonomic Unit) based on the distance matrix using vsearch dgc in Mothur and a cutoff of 0.03. Archaeal OTUs contained abundantly unclassified Archaea. All unclassified archaeal OTUs that contained at least 100 sequences were compared to the nonreduntant nucleotide sequence database using the Basic Local Alignment Search Tool (blast) blastn of the NCBI (National Center for Biotechnology Information) [28]. All OTUs that were assigned to bacterial lineages were removed from further analyses.

Chimeric sequences in the dereplicated ITS sequence data were identified with vsearch in Mothur and were removed. The fungal ITS sequences were classified using the unmodified UNITE ITS database (version 8.2) [29–31]. Sequences that were not classified as fungi were removed. The unaligned ITS sequences were clustered in to OTUs using vsearch and a cutoff of 0.03.

The analyzed sequence data was extracted as biom tables for subsequent alpha- and betadiversity analyses. Taxonomy summaries were made in QIIME version 1.9 [32] (summarize_taxa_through_plots.py). The relative abundance of microbial OTUs and taxonomy levels in the samples was visualized using the ggballoonplot function of the ggpubr package [33] in R and the core microbiome was extracted in Mothur with get.coremicrobiome command [25].

2.7. Metagenomes

Five samples from both sampling times that showed high number of bacterial 16S rRNA genes with qPCR were chosen for shotgun sequencing. The DNA of selected sampling points was submitted to multiple displacement amplification (MDA) using the Illustra Genomi Phi v2 DNA amplification kit (GE Healtcare). Two µL aliquots of each replicate DNA extract/sample were mixed, whereafter the mixture was portioned into two separate 2 µL portions per sample for the MDA reactions. The 2 µL DNA extracts were mixed with 18 µL amplification buffer in 250 µL PCR tubes and heated in a PCR machine for 3 min at 95 °C. The reactions were briefly cooled on frozen (−20 °C) cooling blocks, and 18 µL reaction buffer and 2 µL enzyme mix was added to the reactions. The MDA reactions were incubated at 30 °C for 2 h, where after the enzymes were inactivated by 1 min at 65 °C. The reactions were cooled and the DNA concentration was measured from 1/10 dilutions of the amplified DNA using the Qubit 2.0 Fluorometer (Fisher Scientific). If the MDA reaction was successful, the replicate reactions were combined and the amplified

DNA was purified with the NucleoSpin gDNA Clean-up kit (Macherey-Nagel) and eluted in 50 µL elution buffer. The DNA concentration of the purified MDA DNA was re-checked using the Qbit 2.0 Fluorometer and the OD of the MDA DNA was checked using the NanoDrop-1000 spectrophotometer (ThermoFisher Scientific, Waltham, MA, USA). The contamination level of the samples was deemed low as the DNA amount of the MDA treated samples was 1000x higher than that of the negative reagent controls. A total of 500 ng MDA DNA per sample was sent to Eurofins for 2 × 150 bp paired-end sequencing on the Illumina HiSeq-2000.

Detailed analysis of the metagenomic sequence data is presented in Prosedure S1. Briefly, the sequence quality was checked using the Fastqc v. 0.11.9 [34], the paired reads were merged using the SeqPrep software v. 1.2 [35] and trimmed with Trimmomatic v. 0.39 [36]. The sequence data was co-assembled with the MEGAHIT assembler v. 1.2.8 [37] and the data was inputted to anvi'o v. 6.1 [38] for further analysis. Reads were mapped to the co-assembly using Bowtie2 [39]. Taxonomical composition of the identified gene calls was annotated using Kaiju v 1.7.3 using the nr_euk database version 2019-06-25 [40]. Functional annotations were done locally against the ncbi COGs database (latest version 2003-2014), Pfams (v. 32) [41] and with PROKKA v. 1.14.5 [42] on the USEGALAXY.com server and GHOSTKOALA [43] on the KEGG server. The contigs were binned manually in the anvi'o interactive interface and refined manually to remove redundancy and contamination. Completeness and redundancy of the metagenome-assembled genomes (MAGs) was checked by CheckM [44] in anvi'o.

Sulfur, nitrogen and arsenic compound oxidation and reduction, sulfur, iron, copper, zinc, manganese transport and several heavy metal resistance and efflux coding genes were searched and counted from the anvi'o's gene detection data. As a reference, incidences of some main genes related to oxidative phosphorylation, glycolysis and fermentation were also counted. Gene annotations were mainly based on Prokka and GhostKoala and to a minor extent on COG or Pfam.

2.8. Chemical Analyses

In addition to biological analysis, samples were also taken for physicochemical and chemical analysis. The following parameters were measured in situ: specific conductance (SPC), pH, oxidation–reduction potential (ORP), dissolved oxygen (DO), and temperature. ORP measurements used Ag/AgCl as the reference electrode. Immediately after sampling, the above mentioned parameters were measured with the YSI ProDSS multiparameter probe (YSI, Xylem Inc., OH, USA). The probe recorded the readings for 10 min to make sure that equilibrium was obtained. The Water-Oxygen line calculated based on Nernst Equation [45] was used to evaluate the change of ORP–pH profile along the plant and part of water circuit.

For other physicochemical properties and chemical analysis, a two-liter slurry sample was drawn into a clean bucket and analysed after preservation using the methods shown in Table S1.

2.9. Statistical Analyses

Alpha diversity analyses for amplicon sequencing results were calculated in Mothur (summary.single) including the Shannon diversity index, and the Chao out richness estimate (Table S2). The similarity of the archaeal, bacterial and fungal communities between the different sample sites was tested by principal coordinate analysis (PCoA) using the Phyloseq package in R [46]. The analysis was performed using the relative abundance OTU tables. The Bray-Curtis dissimilarity model was used for both analyses. Eigenvalues for the variance explained by the PCoA dimensions were calculated on 9999 random repeats. Based on the PCoA comparisons of original abundance OTU tables including all samples and negative controls, the effect of OTUs found in negative controls was assessed. Samples that grouped close to negative control samples were found to contain less than 90 or 20 sequences in bacterial or archaeal samples, respectively. It was concluded that these

samples were affected by contamination and they were removed from further analyses. In the case of fungal samples, the biggest (>10 sequences) fungal OTUs found from negative control samples may have affected the samples and these OTUs were removed from all samples. Samples with 20 or more fungal sequences left were further analysed similarly as the bacterial and archaeal samples. Environmental factors exhibiting statistically significant effects ($p < 0.01$ or $p < 0.001$ with 9999 permutations) on the microbial communities were identified using the Vegan package [47] in R.

Significant differences in the microbial numbers between the sampling sites was tested with one-way ANOVA and further with Mann-Whitney pairwise tests with Bonferroni corrected p-values and the significant differences between sampling times was tested with two-sample t-test from log transformed qPCR results in PAST version 3.14 [48]. Correlation (Pearson's r) of sulfur metabolism-related genes from the annotated metagenomic detection data between June and November samplings in each sample were tested also in PAST 3.14.

3. Results

3.1. Process Water Chemistry

In situ physicochemical measurements (Table 1) and the chemical compound concentrations (Figures 3 and 4) were analyzed to characterize the process steps and to be able to evaluate their effects on microbiological communities. The temperatures of the samples varied between 14.4 and 36.1 °C (Table 1). In both samplings, the Santa Clara reservoir raw water had the lowest temperature. The mine and process waters had much higher temperatures due to the energy provided by the process, and the Santa Clara only contributes a small portion (less than 10%) of the process water since the mine recycles water. The lowest process temperatures below 20 °C were measured from the Cu Thickener Overflow in November and from ETAM Out samples both in November and in June. The highest temperatures of above 36 °C, were found from the Cu RC Final Tailings and Cu Rougher Feed in June. The seasonal temperature difference was less than 2 °C in Zn plant samples and 4–5 °C in the Cu plant samples. Oxygen levels in the samples were lowest in both Zn Rougher Feed samples (0.1 to 1.2 mg L^{-1}) and the highest in the ETAM Out sample in June (12.9 mg L^{-1}).

Table 1. The in situ measurements of the studied process samples in June and November samplings 2018; no samples were available from the TAI water. SPC, specific conductance; DO, dissolved oxygen; ORP, oxidation–reduction potential; N.A, not analysed.

Samples	T	SPC	pH	DO	ORP
	°C	mS cm^{-1}		mg L^{-1}	mV SHE
			June		
Zn Rod Mill Feed	27.3	7.0	6.4	5.5	182
Zn Rougher Feed	35.0	4.6	6.8	1.2	245
Zn RZ Tails	33.2	6.3	6.9	3.9	387
Cu Rod Mill Feed	27.5	7.0	6.5	5.5	190
Cu Rougher Feed	36.0	4.4	10.0	1.8	72
Cu RC Final Tailings	36.1	5.2	10.2	2.9	200
Cu Concentrate Thickener Overflow	25.2	6.8	6.7	6.3	320
Paste Thickener Overflow	31.0	6.9	9.4	3.8	251
ETAM in	22.2	5.1	8.6	8.9	319

Table 1. *Cont.*

Samples	T	SPC	pH	DO	ORP
	°C	mS cm^{-1}		mg L^{-1}	mV SHE
			June		
ETAM out	19.1	6.6	9.5	12.9	290
Santa Clara	23.2	0.3	8.8	6.3	360
			November		
Zn Rod Mill Feed	26	7.3	7.0	5.4	272
Zn Rougher Feed	33.3	5.5	6.8	0.1	259
Zn RZ Tails	33.0	5.0	6.7	4.1	276
Cu Rod Mill Feed	26.2	7.5	7.0	5.4	270
Cu Rougher Feed	30.6	4.7	8.8	5.1	141
Cu RC Final Tailings	32.2	5.2	9.4	4.4	133
Cu Concentrate Thickener Overflow	N.A	N.A	N.A	N.A	N.A
Paste Thickener Overflow	27.2	7.4	9.4	6.9	214
ETAM in	22.5	6.6	8.1	8.0	336
ETAM out	17.4	7.0	7.4	6.9	341
Santa Clara	14.4	0.3	7.9	7.6	401

The pH in the zinc plant samples (Zn Rougher Feed and Zn RZ Tails) was generally lower than in the samples from the copper plant (Cu Rougher Feed and Cu RC Final Tailings). This was a direct consequence of the lower pH set for the zinc plant than for the copper plant. Overall, pH values observed in November at the copper plant and in the water circuit samples were around one unit lower than in June except for the Paste Thickener Overflow and Cu Rod Mill samples (Figure 2B). The pH in the water circuit samples ranged from 7.4 to 9.5, the ETAM Out samples having the biggest difference between the samplings (Table 1). No significant changes were observed in terms of ORP value for either sampling campaign (except for Cu Rougher Feed where the difference was higher than 50%). The redox potential was the lowest in Cu Rougher Feed samples in both samplings (72 and 141 mV SHE) and in Cu RC Final Tailings (133 mV SHE) in November. The highest redox potential was measured in Zn RZ Tails in June (387 mV SHE) and in all ETAM samples (290–341 mV SHE) and in the Santa Clara water (401 mV SHE) in November.

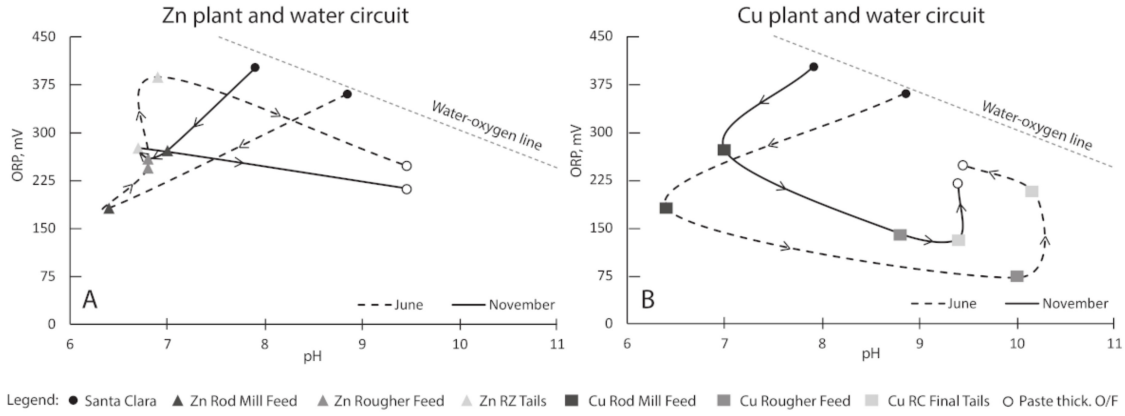

Figure 2. ORP–pH curves from samples with in situ measurements from water ciruits within (**A**) the Zn plant, (**B**) the Cu plant.

The ORP–pH data (Figure 2) determine where chemical reactions (e.g., oxidation–reduction; precipitation) are occurring and whether there are any major changes in types of reactions in the plants between the two sampling campaigns. If the ORP–pH curve is parallel to the water–oxygen line, the water is in equilibrium. If the ORP–pH curve is perpendicular to the water–oxygen line, then oxidative reactions have occurred. Figure 2 shows that the ORP–pH line from the Santa Clara water to the Zn Rod Mill Feed is perpendicular to the water–oxygen line. Additionally, since the Zn Rod Mill Feed consists mostly of a shortly recycled stream from the paste thickener plant, it indicates that the whole system is oxidative. In the case of the Zn plant, the change from Zn Rod Mill Feed to Zn Rougher Feed is perpendicular to the oxygen–water line for both sampling campaigns. Therefore, it is likely that oxidative reactions occurred in the grinding circuit of the Zn plant. This was not the case for the Cu plant, as the lines from Cu Rod Mill Feed to Cu Rougher Feed are parallel to the water–oxygen line for both samplings. In June, oxidative reactions occurred in the flotation circuit of both copper plant and zinc plant, whereas in November, the water equilibrium was maintained. The changes of pH from the Zn plant to the paste plant are attributed to the addition of lime in the tail plant as a coagulant aid. Such a change is not pronounced in the case of the Cu plant since the Cu plant is operated at higher pH.

The profiles of major and minor chemical compounds, respectively, throughout the plants and water circuit are presented in Figures 3 and 4. The minor chemical compounds are defined as those that contribute, on average, less than 1% to the TDS. Since the Santa Clara water is freshwater from the local river, its composition differs greatly from the mine waters, characterized by a low concentrations of both minor and major chemical compounds.

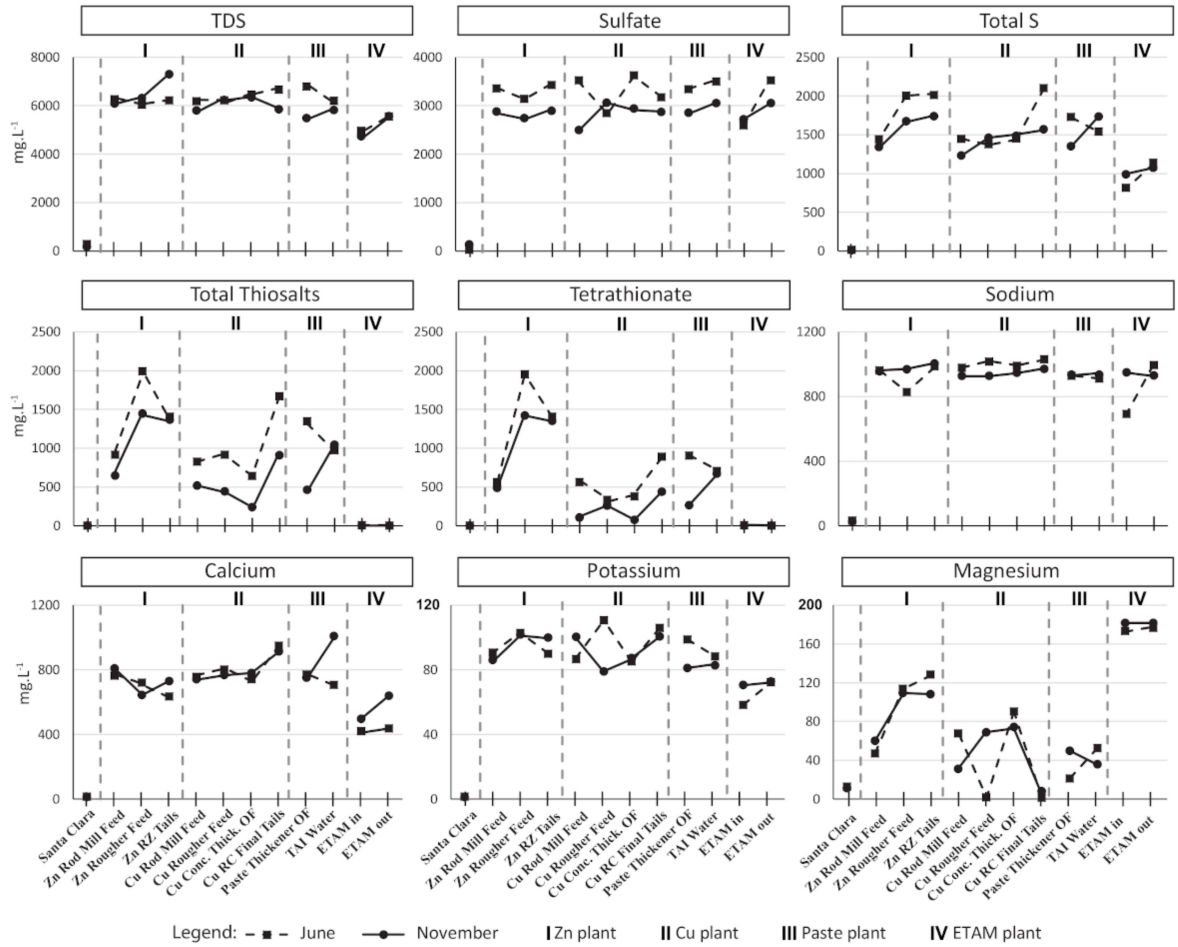

Figure 3. The profiles of major chemical compounds throughout the plants and water circuit. TDS, total dissolved solids.

The mine waters (from the plants and the water circuit) were characterized by a high amount of TDS (around 6000–7000 mg L^{-1}). Since the plants process high-grade sulfide ore, the sulfate concentration in the mine waters was high, varying between 2800 and 3500 mg L^{-1}. The concentration of calcium varied throughout the plants and water circuit. The highest concentration of calcium was observed in the Cu RC Final Tails and the Paste Thickener Overflow samples. This reflects the fact that lime is used to increase pH in the Cu plant and as a coagulant in the tail plant. On average, the concentration of calcium in the mine waters varied around 800 mg L^{-1}, indicating that the mine waters were saturated with gypsum.

The concentration of thiosalts fluctuated highly through the plants and water circuit. However, even though there was a variation between the samplings, the pattern profiles remained the same (Figure 3). The concentrations of sodium and potassium did not vary between the two sampling campaigns, as there were on average only 9% and 8% differences in sodium and potassium concentrations between the samplings, respectively. The profile of sodium remained constant throughout the plants and the water circuit; instead, the concentration of potassium tended to increase during milling at both plants. The concentration of magnesium was highest in the ETAM In and Out waters, and overall the concentration of magnesium was lower in the Cu plant than in the Zn plant.

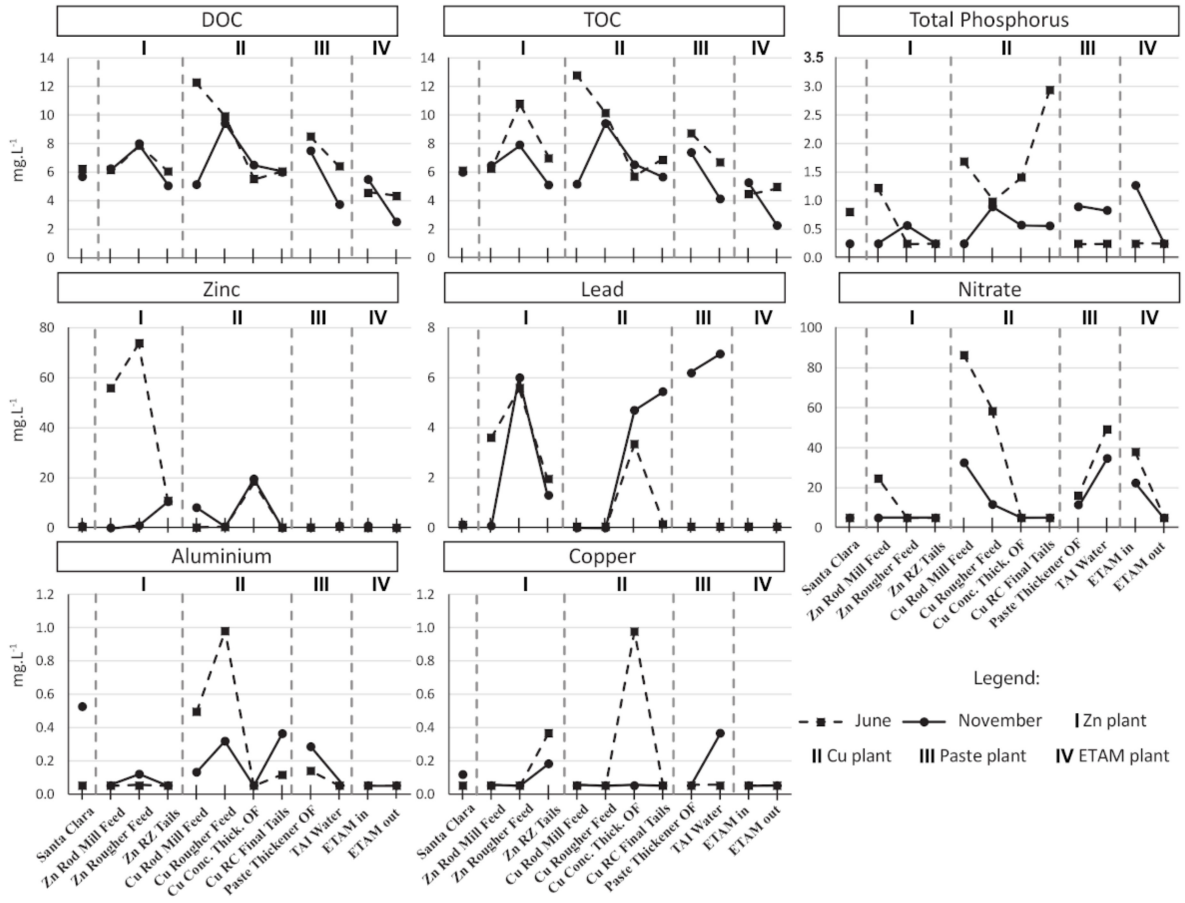

Figure 4. The profiles of minor chemical compounds throughout the plants and water circuit. DOC, dissolved organic carbon; TOC, total organic carbon.

In terms of minor chemical compounds, total organic carbon (TOC) and dissolved organic carbon (DOC) had very similar profiles and concentrations (Figure 4). The only difference was observed in the Zn RZ Tails in June where the TOC concentration was 20% higher than the DOC concentration. In the November sampling campaign, peaks in the

organic carbon concentrations were observed in the Zn RZ Tails, the Cu RC Final Tails and the Paste Thickener Overflow samples. In the June sampling campaign, another organic carbon peak was observed in the Cu Rougher Feed sample. Phosphorus concentrations varied greatly between the sampling campaigns. Elevated carbon and phosphorus concentrations are likely a consequence of flotation and thickening reagent additions. During both sampling campaigns, three nitrate concentration peaks were observed from the Zn and Cu Rougher Feeds, the ETAM In, and the ETAM Out samples. The concentrations of metals in the process water were generally lower than the limit of detection, except for lead. High concentration of lead was observed in both the copper plant and the zinc plant. In November, a high concentration of lead was also observed in the water circuit (TAI Water, Paste Thickener Overflow and ETAM In waters). The variations in metal concentrations are difficult to interpret since several factors, such as ore mineralogy, oxidation degree and variation of pH, can have an effect.

3.2. Estimated Sizes of the Microbial Populations

Bacterial, archaeal and fungal community sizes were estimated with qPCR to be able to see differences between the samples and the two sampling occasions. Bacteria were present in all samples. The most bacteria were detected in November Zn Rod Mill Feed and ETAM In samples with over 1×10^7 bacterial 16S rRNA gene copies mL^{-1} (Figure 5). Bacterial gene copy counts differed statistically significantly ($p < 0.03$) in all except the Cu RC Final Tails and Paste Thickener Overflow samples between the two samplings. However, there was no clear trend of either sampling harbouring more microorganisms in the samples. The ETAM In and Out samples showed the greatest differences between samplings, as the gene copy counts were over one and up to two orders of magnitude higher in November. The Santa Clara reservoir water contained about one order of magnitude less bacterial 16S RNA gene copies mL^{-} than the Industrial Water (TAI Water). There were four samples, the Rougher Feeds and Tail samples from both the zinc and copper plants, where only low amounts of DNA was extracted and thus only low gene copy levels were detected in the qPCR with the targeted bacterial, archaeal and fungal marker genes. Nevertheless, microscopy showed abundantly microorganisms present also in these samples (Figure 6). It was not possible to quantitate microbial counts with microscopy as the cells were largely attached to the mineral particles and part of the cells remained under these particles and could not be counted.

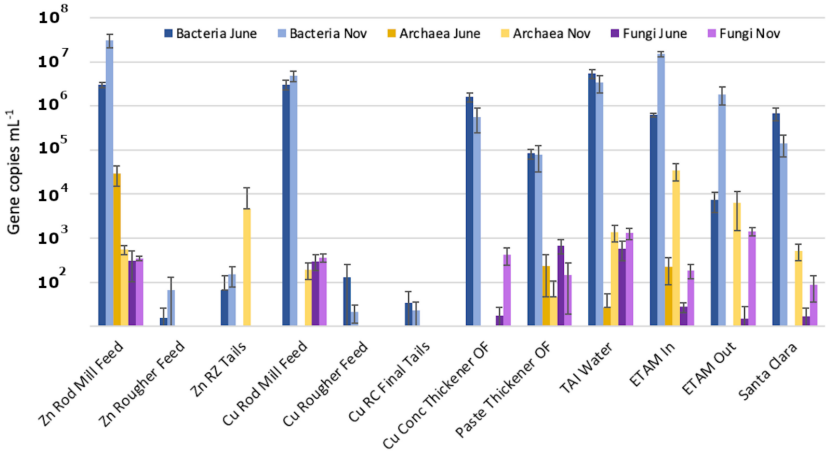

Figure 5. The average numbers of bacterial and archaeal 16S rRNA gene copies mL^{-1}, and fungal 5.8S rRNA gene copies mL^{-1} in the June and November samplings. Each bar is the average of three parallel qPCR reactions of three replicate samples and the error bars display standard deviation. The y-axis displays number of gene copies mL^{-1}.

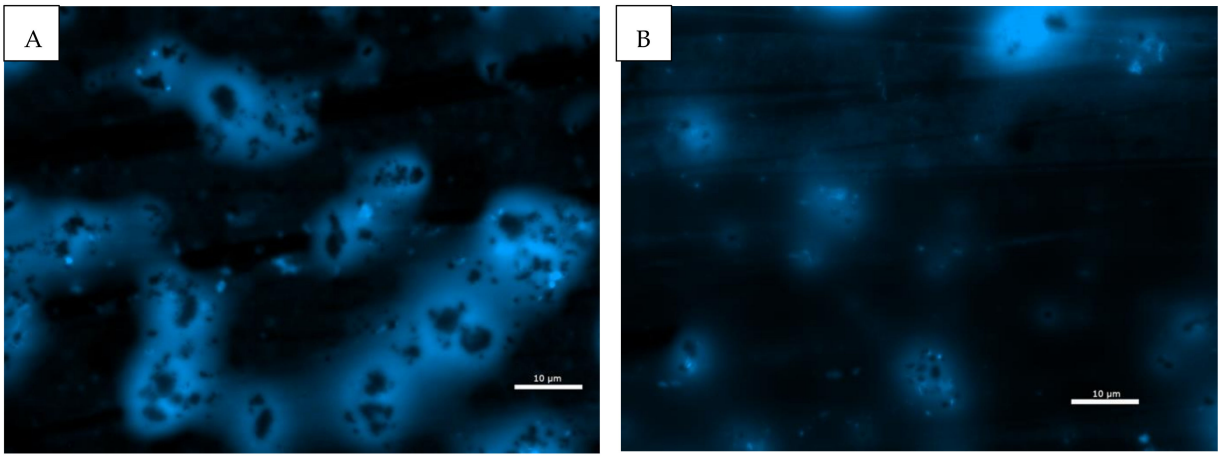

Figure 6. Epifluorescence image of DAPI (4′,6-diamidino-2-phenylindole) stained (**A**) Zn RZ Tail June sample and (**B**) Cu Rougher Feed November sample. Cells appear as bright blue spots and residual stain as paler blue, especially around the black mineral particles. The scale bar indicates 10 µm.

Archaeal 16S rRNA gene copy counts ranged from below the detection limit to 3.4×10^4 mL^{-1}. The ETAM In sample in November and the Zn Rod Mill Feed sample in June had the highest archaeal gene copy numbers. Archaea were more frequently detected in November samples than in June samples where archaea were below the detection limit in several samples. Differences between samplings were great in all samples containing archaea. However, no clear trend in samples of either sampling occasion having more archaea was observed (Figure 5).

Fungi were detected in all other samples except for those with low amounts of extracted DNA, and in general fungi were more common in November samples than in June samples. The fungal 5.8S rRNA gene copies varied between 7 and 1.4×10^3 mL^{-1} and the ETAM Out samples had the highest number of fungal 5.8S rRNA gene copies, with two orders of magnitude higher amounts in the November sample.

3.3. Microbial Communities

The amplicon sequencing produced only low sequence counts from especially Rougher Feed and Tails samples, despite efforts to re-sequence the amplicon libraries of these samples. The number of bacterial sequence reads, average of three replicate samples, ranged from 18 from the zinc plant RZ Tails sample in June to 16,496 from the Santa Clara water in November (Table S2). In general, samples with a low amount of extracted DNA produced low sequence read counts (the Rougher Feeds and the Tails samples), which also affected the OTU numbers detected. The same trend was visible in the archaeal results as low number or no sequences were obtained from the Rougher Feeds and the Tails samples. In the case of fungi, the trend was not as apparent for sequence read counts although the number of OTUs was lower in Rougher Feed and Tails samples than in the other samples. According to the Chao1 richness estimate, the coverage of detected bacterial and archaeal OTUs was less than 50% in most of the samples. Fungal sequencing succeeded best, but also here only around two thirds of the Chao1 estimated number of fungal OTUs were detected. The Shannon diversity index was higher in November than in June samples with all studied microorganism groups in water circuit samples TAI Water, ETAM In and Out samples and the Santa Clara water reservoir sample. However, it is likely that the low sequence read counts affected the Shannon index and only the bacterial data is relatively reliable. In the other samples there was no trend between samplings in the diversity index values, partly also affected by the low sequence counts.

3.3.1. Bacteria

The amplicon sequencing showed that the bacterial communities consisted mostly of Proteobacteria (Figure S1) and especially of different Gammaproteobacteria (Figure 7). All the different process water samples studied harboured high relative abundances of reduced sulfur species oxidising bacterial genera, such as *Thiovirga*, *Thiobacillus* and *Halothiobacillus*. Sulfur oxidisers were also present in the raw water from the Santa Clara reservoir, but their relative abundance was much lower than in the different process water samples. The raw water from the Santa Clara had also clear seasonal difference, changing from *Alishewanella*, *Pseudomonas* and *Thiovirga* dominated to Actinobacteria (CL500-29 marine group, Sporichthyaceae) and SAR11 dominated communities in November. *Thiovirga* dominated in the zinc plant Rod Mill and Rougher Feed samples in June and November whereas, the relative abundance of *Thiobacillus* was high in the copper plant Rod Mill Feed and Cu Concentrate Thickener Overflow samples. In addition, *Halothiobacillus* in Cu Rod Mill Feed and another sulfur oxidizer, *Azospira*, in Cu Concentrate Thickener Overflow November samples had high relative abundances. Copper plant Rougher Feed samples harboured all main sulfur oxidisers found in these samples, namely, *Thiobacillus*, *Thiovirga* and *Halothiobacillus*. The dominant bacteria in the copper RC Final Tails sample was different as the relative abundance of the three main sulfur oxidizers was lower and groups such as *Thermithiobacillus, Pseudomonas* and Burkholderia-Caballeronia-Paraburkholderia were the most prominent groups detected. In the Paste Thickener Overflow samples *Thiovirga* dominated again but other bacterial groups such as *Pseudomonas*, *Alishewanella* and Sporichtyaceae were also relatively prominant. The relative abundance of different bacterial groups both in June and November in ETAM In water, going to the mine water treatment plant, were very similar. The most dominant bacterial group was *Thiovirga* but also *Acinetobacter*, *Pseudomonas*, *Thiobacillus* and *Alishewanella* were relatively abundant. Water coming out of the water treatment plant (ETAM Out) had quite different bacterial profiles in June and November regardless of the similarities found in the ingoing water samples. In June the ETAM Out water was dominated by *Thiovirga* only. In November, the ETAM Out water had several prominent bacterial groups including *Thiovirga*, *Acinetobacter*, *Hydrogenophaga*, *Algoriphagus*, *Spirosomaceae*, *Rickettsiaceae* and *Sphingomonadaceae*. In the Industrial Water TAI, some differences in the bacterial community composition between the samplings were detected. In June the water contained high relative abundances of *Thiovirga*, *Thiobacillus*, *Halothiobacillus*, *Ferritrophicum*, *Pseudomonas*, *Alishewanella* and *Diaphorobacter*. In contrast, the November TAI Water had a wider diversity as in addition to the prominent bacterial groups in June, also Rhodanobacteraceae and *Telmatospirillum* were part of the main bacterial community. The bacterial coremicrobiome of different process waters consisted of *Thiovirga*, *Thiobacillus*, *Halothiobacillus*, *Pseudomonas* and *Diaphorobacter* OTUs that were found at least with 1% relative abundance in half of the samples.

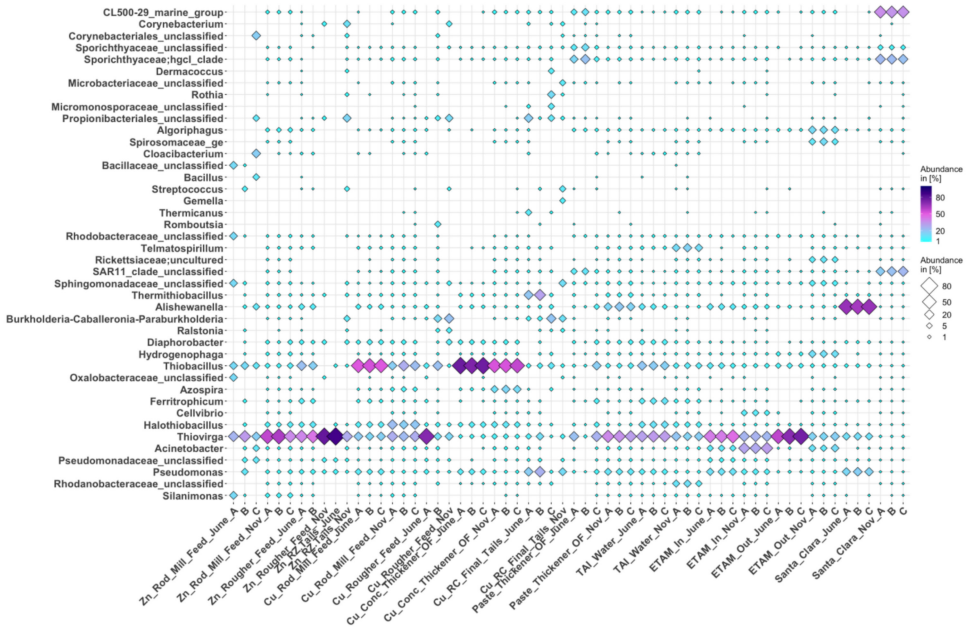

Figure 7. Bacterial genera containing at a minimun 5% relative abundance in at least one sample. Sampling was performed in June and November 2018 originally with triplicate samples but only samples with over 90 reads are shown. The June Cu Rougher Feed sample represents water phase (A) and a mixture of water and solids in the sample (B). The bacterial genera are presented on the left of the graph and the relative abundances of the different genera in each sample are represented by a gradient shading and size of the diamonds.

3.3.2. Archaea

Clearly the biggest group of archaeal sequences remained as unclassified archaea (Figure 8) by the amplicon sequencing. The most prevalent of the identified archaeal classes included ammonia oxidizing Nitrososphaeria of the phylum Crenarchaeota and Thermoplasmata of the Thermoplasmatota phylum.

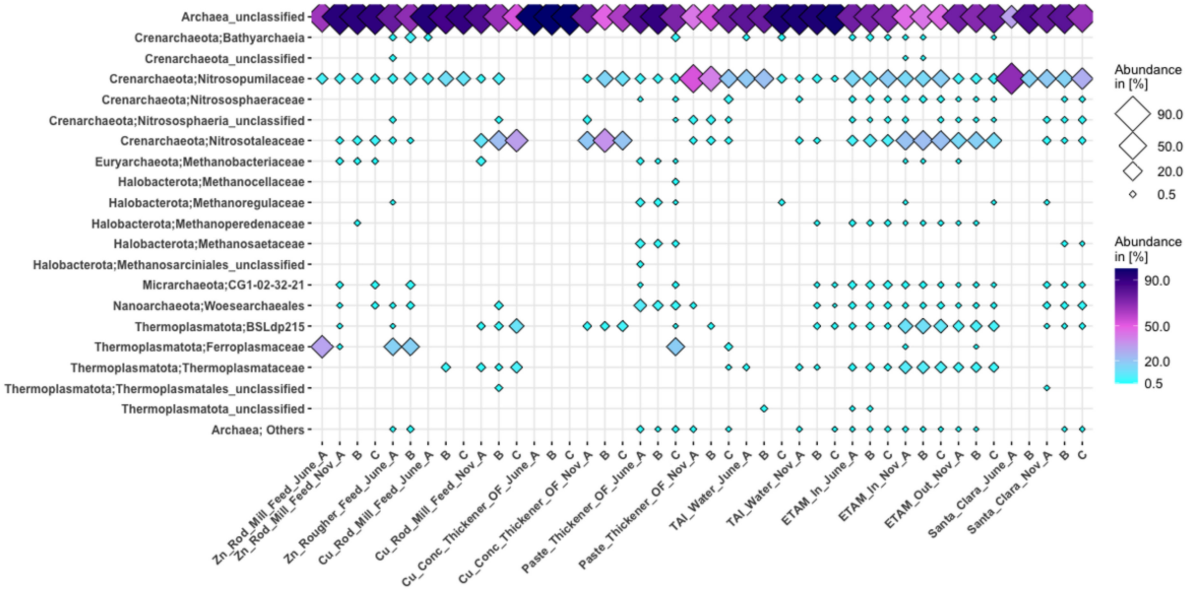

Figure 8. Archaeal classes containing at a minimum 1% relative abundance in at least one sample and other low abundance classes are combined into Archaea; Others. Sampling was performed in June and November 2018 originally with triplicate samples but only samples with over 20 reads are shown. The archaeal genera are presented on the left of the graph and the relative abundances of the different genera in each sample are represented by a gradient shading and size of the diamonds.

3.3.3. Fungi

A large part of the fungal ITS amplicon sequences obtained belonged to unclassified fungal groups that formed a high share of the sequences especially in the June samples of Zn Rougher Feed, Cu Concentrate Thickener Overflow, Paste Thickener Overflow and ETAM In water (Figure 9). In addition, in both the copper Rod Mill Feeds in June and November the share of unclassified fungi was high. The Santa Clara water was the only sample where the share of unclassified fungi was higher in November than in June. Two fungal phyla with high relative abundance were Ascomycota and Basidiomycota. Additionally, some Chytridiomycota were found. In general, there seemed to be more fungal classes present in the November than in June samples. There were also clear differences in the relative abundances of fungal classes in some of the replicate samples (Zn Rod Mill Feed June, Zn RZ Tails June, Cu Rougher Feed June and November) likely due to the low sequence counts. The Ascomycota classes Dothideomycetes, Eurotiomycetes and Sordariomycetes were most often detected. Basidiomycota class Agaricomycetes was also a common class in the samples and the class Malasseziomycetes was especially prominent in both zinc and copper Tails samples.

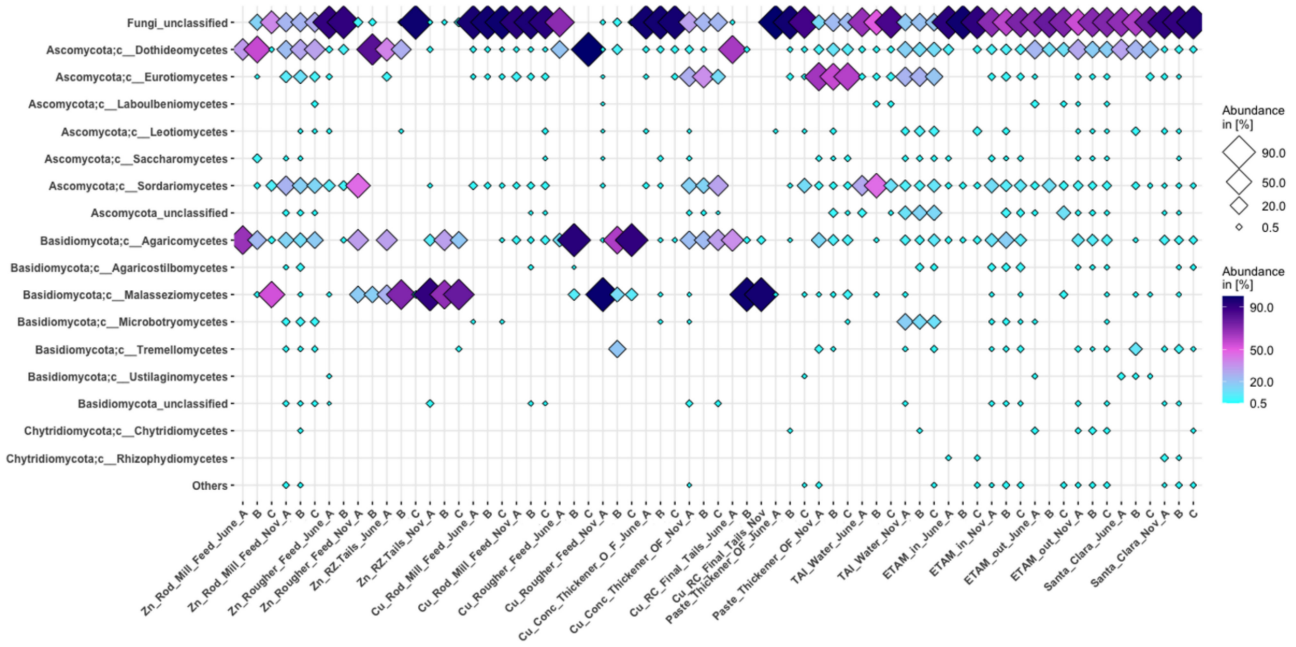

Figure 9. The relative abundance of the main fungal classes, other minor abundance classes are combined into Others. Sampling was performed in June and November 2018 originally with triplicate samples but only samples with more than 20 reads are shown. The June Cu Rougher Feed sample represents either water phase, mixture of water and solid, or solids. The fungal classes are presented on the left of the graph and the relative abundances of the different classes in each sample are represented by a gradient shading and size of the diamonds.

3.4. Metagenomics

3.4.1. Metagenomic Data

The number of paired end raw sequence reads varied between 11.35 and 20.12 Mb per sample and 11.26 and 19.96 Mb trimmed reads per sample (Table S3). The minimum contig length was set to 2.5 Kb and the total length of this co-assembly was 182 Mb with a maximum coverage of 8× (Table S4). The total number of contigs over 2.5 Kb in length was 21,027. The N50 of the co-assembly was 13.1 Kb and the longest contig was 342 Kb. The total number of predicted genes by Prodigal was 149,782 and the proportion of trimmed sequence reads mapped back to the co-assembly was between 55.7% and 88.6%. More details are found in the Procedure S1.

3.4.2. Metabolism

The abundance of identified genes is based on anvi'o's term "detection", which indicates the proportion of the sequence of a predicted gene that is covered by the mapped reads, i.e., 0 to 1. If the "detection" for any specific gene is 1 the whole gene sequence can be found back-mapped from the sequence reads, whereas if the "detection" is only 0.5, only 50% of the gene sequence is covered by the sequence reads. The "detection" does not account for the coverage of the gene. It was assumed that a high "detection" value for a gene was equal to good coverage of the gene, as the total coverage was only 8 times at most. Sulfur and nitrogen compound oxidation and reduction abilities (Figure 10), glycolysis, oxidative phosphorylation, pentose phosphate, Entner–Doudoroff pathway and some fermentation-related genes (Figure S2) and heavy metal resistance genes (Figure 11) were studied from the gene "detection" data.

The Sox system for thiosulfate oxidation together with flavocytocrome C sulfide dehydrogenase (*fcc*) and sulfide:quinone oxidoreductase (*sqr*) genes dominated the reduced sulfur compound oxidation in the studied communities. The abundance of the *soxCD* complex was lower than that of other sox components which indicates that part of the sulfur oxidizers were lacking this *soxCD* complex. However, the formed sulfur could be futher oxidized through the dissimilatory sulfite reductase system (*dsrC*, *dsrAB*) which seemed an alternative route to *soxCD*. Thiosulfate oxidizing thiosulfate dehydrogenase (*tsdA*) gene was also abundantly found but tetrathionate (tetrathionate hydrolase, *tth*) and thiocyanate (*scn*, thiocyanate hydrolase) oxidizing potential was low in the samples. Sulfur trafficking genes, especilly *dsrE/F* family and *tusA* were abundantly found in all samples indicating sulfur a significant role in the community metabolism. There was also potential for several sulfur compound reduction reactions present (*dsrABC*, *sat*, *aprAB*, *ttrABC*, *phsAC*) in the communities in case of oxygen-poor or anaerobic environments occurring in some parts of the process and assimilatory sulfate reduction to sulfide. The profiles of sulfur-related genes from the same samples in June and November resembled each other with correlations from 0.871 (ETAM Out) up to 0.993 (Zn Rod Mill Feed) ($p < 0.5 \times 10^{-15}$). However, there were a difference in gene "detection" counts especially between seasons in the ETAM Out samples (higher in November) and in Cu Rod Mill Feed samples (higher in June). This was not related to mapped read counts as those were higher for samples with lower gene "detection" counts. The mapped read counts were the highest for both the Cu Concentrate Thickener Overflow samples but the genes "detected" related to sulfur, nitrogen or energy metabolism (Figure 10 and Figure S2) were lower than for most other samples. Generally, all the studied energy metabolisms and not only specific metabolism type such as sulfur metabolism was lower in Cu Rod Mill Feed November, in both Cu Consentrate Thickner Overflow samples and ETAM out June sample than in other samples.

The mean "detection" level of S-compound and sulfide oxidation genes (*SoxXYZAB*, *FccAB*, *sqr*) was around half of the mean "detection" level of the first and the last step of the oxidative phosphorylation or the three-carbon core compound glycolysis genes (Figure 10 and Figure S2). "Detection" level of genes related to fermentation as an end process of glycolysis was clearly lower than that of S-compound and sulfide oxidation genes. In addition to genes for glycolysis, genes for other glycolytic pathways such pentose phospate and Entner–Doudoroff pathways were detected abundantly (Figure S2) but less than for glycolysis.

The assimilative nitrate reduction (*nasA*) gene was the most abundantly found gene of the nitrogen metabolism (Figure 10). In contrast, the *nasB* subunit was not detected which is confusing compared with the *nasA* gene abundance. Dissimilative nitrate oxidation/nitrite reduction (*narGHI*/*nxrAB*)-related genes and nitric oxide (*norBC*) and nitrous oxide (*nosZ*) reductive genes were also abundantly detected. Nitrite dissimilatory reduction to ammonia (*nirBD*) genes were also abundant and nitrite reduction in denitrification to nitric oxide (*nirS, nirK*) genes were found slightly less. In addition, nitrogenases (*nifDK*, *nifH*) for elemental nitrogen (N_2) fixation were present. Only the gamma subunit of the ammonia monooxidase (*amoC*) was detected in the samples. Differences between June and November

samplings were similar as in the case of sulfur metabolism. The mean "detection" level of the main nitrogen metabolism genes was slightly lower than that of the main S-compound genes detected.

Heavy metal-related genes were detected abundantly in all samples, which was obvious compared to prevalence of antibiotic resistance genes (Figure 11). Similarly to the cases of sulfur, nitrogen and general energy metabolism, the lowest gene abundancies were found in both Cu Concentrate Thickener Overflow samples and in the June ETAM Out sample, and in the November Cu Rod Mill Feed sample. Copper, zinc, nickel, cobalt and chromium are essential trace elements required by numerous metalloenzymes in microorganisms. However, in high concentrations they are toxic for microbial cells and need to be controlled. Several heavy metal resistance protein genes were detected, most abundantly multimetal cobalt-zinc-cadmium/cobalt-nickel and copper resistance proteins. Genes for arsenic, mercury and chromate resistance proteins were also abundantly detected in addition to Lead-cadmium-zinc-mercury resistance gene. Some antibiotic resistance genes were detected, especially for β-lactams and macrolides.

3.4.3. Metagenome-Assembled Genomes (MAGs)

There were 20 manually binned MAGs that were over 70% complete (Figure S3). The most complete (98.6%) was a Thiomicrospirales MAG that contained a high percentage of mapped reads from especially both June and November Zn Rod Mill Feed and ETAM out samples. This MAG contained almost all 16S rRNA sequences (99.9%) that were classified as *Thiovirga* based on 16S rRNA amplicon sequencing. However, the 16S rRNA sequences in the NCBI blast® with the nucleotide collection (nr/nt) gave equal identification with several uncultured bacteria and a few *Thiovirga* sp. The real identity of this bacterial MAG remained unknown, one reason being that no genome of *Thiovirga* sp. has yet been published. It is possible that this MAG does not belong to *Thiovirga* but some other yet unidentified sulfur oxidizing species as it contained *SoxXYZABD* genes, although the SoxC gene remained unidentified. In addition, the MAG contained genes for sulfide oxidation (*sqr*, *fccAB*), an incomplete assimilatory sulfate reduction pathway (*CysNDCJ*) and sulfur trafficking genes *tusA*, *dsrE/F*. It also had dissimilatory nitrite reductase genes (*NirBD*). Genes for the first and the last step of the oxidative phosphorylation and for glycolysis three-carbon core compounds were detected but no genes for pentose-phosphate or Entner–Doudoroff pathway were found. In addition, there were many heavy metal resistance genes (*czcABC*, *copABRS*, *arsCR*, *merR*, *chrA*) and even tetracycline resistance gene (*tetA*) present in the MAG.

Other MAGs that contained a high percentage of mapped reads from many or at least one sample were classified as *Halothiobacillus neapolitanus*, that was especially common in the Cu Concentrate Thickener Overflow samples, *Halothiobacillus* sp., recruiting reads especially from the June TAI Water sample, *Acinetobacter* sp. common in the November ETAM Out sample, *Thiobacillus* sp. with high read recruitment from the Cu Concentrate Thickener Overflow samples, and *Limnobacter* sp. with high read recruitment from the ETAM Out June sample.

Sulfur metabolism	Genes	Zn Rod mill feed June	Zn Rod mill feed November	Cu Rod mill feed June	Cu Rod mill feed November	Cu Concentrate thickener O/F June	Cu Concentrate thickener O/F November	TAI water June	TAI water November	ETAM Out June	ETAM Out November
S-compound oxidation	*SoxX*	31	33	25	16	11	13	32	31	4	16
	SoxY	12	15	9	5	3	7	13	13	3	8
	SoxZ	13	16	12	8	5	8	13	12	5	10
	SoxA	31	33	25	16	11	13	32	31	4	16
	SoxB	22	23	26	10	11	10	23	18	5	11
	SoxC	3	6	4	3	1	2	3	4	2	4
	SoxD	3	6	5	5	3	3	4	6	3	5
Sulfide oxidation	*FccA*	8	7	7	6	3	6	8	9	1	3
	FccB	21	20	19	11	9	10	21	18	3	9
	sqr	57	58	67	30	32	33	62	57	10	29
Sulfur oxidation	*hdrA2*	1	1	1	0	1	1	0	2	0	2
	hdrB2	8	8	8	3	4	3	7	9	0	6
	hdrC1/C2	1	1	2	0	1	1	1	2	0	2
	hdrD	5	4	4	2	0	0	5	4	1	4
	ETHE1	5	5	4	3	2	3	5	4	1	4
(Sulfite reduction)	*dsrA*	11	10	10	4	2	3	12	9	1	3
	dsrB	7	7	7	3	2	3	8	7	1	3
	dsrC	48	41	47	25	15	20	52	40	1	10
Sulfite oxidation	*aprA*	11	10	10	6	4	7	11	10	0	8
(APS reduction)	*aprB*	8	7	8	3	1	2	9	8	0	4
(Sulfate reduction)	*sat*	10	8	13	4	9	5	9	8	0	3
	soeA	10	10	9	3	4	3	10	9	2	3
	soeB	11	11	12	4	5	6	11	11	3	5
	soeC	10	11	11	5	4	4	10	10	2	4
	sorAB	1	1	1	1	0	0	1	0	0	1
Sulfate reduction	*PAPPS*	1	1	0	1	0	0	0	0	1	1
(assimilatory)	*cysD*	24	28	26	16	11	12	30	26	7	24
	cysNC	16	15	17	8	5	6	17	15	3	10
	CysN	9	11	9	6	5	6	11	11	7	8
	CysC	14	20	16	10	7	8	18	19	4	11
	CysH	18	24	24	11	13	10	19	18	10	19
	CysI	8	9	9	3	4	4	8	6	4	8
	CysJ	23	20	28	13	14	11	26	25	5	11
Thiosulfate oxidation	*doxAD*	1	1	4	0	3	0	1	3	0	2
	tsdA	20	17	21	9	10	10	21	19	3	6
Tetrathionate oxidation	*tth*	0	1	2	1	1	1	1	0	0	0
Thiocyanate oxidation	*scnA*	1	2	1	1	1	1	1	1	0	1
	scnB	1	1	1	2	1	1	1	1	0	1
	scnC	3	4	3	3	2	2	3	3	1	2
Sulfur trafficking	*tusA*	44	38	58	22	33	26	44	47	2	18
	dsrE2	9	7	10	5	6	5	11	7	2	2
	dsrEF	119	119	138	68	75	73	123	125	14	55
	dsrH	7	8	6	5	3	4	8	8	1	6
	rhd	4	4	4	2	1	1	5	4	0	1
Tetrathionate reduction	*ttrA*	16	17	20	7	11	5	18	11	3	7
	ttrB	27	31	31	13	14	12	32	26	3	13
	ttrC	7	9	8	4	6	5	9	6	2	5
Thiosulfate reduction	*phsA*	4	5	6	2	3	2	4	4	0	2
	phsC	6	7	7	4	2	3	7	6	1	1
Nitrogen metabolism											
Ammonia oxidation	*amoC*, no A/B	7	9	12	5	6	4	8	7	4	10
Nitrate reduction/	*narG/nxrA*	22	24	22	10	8	9	24	21	2	12
Nitrite oxidation	*narH/nxrB*	16	22	18	7	8	9	19	18	1	11
(dissimilatory)	*narI*	24	26	23	8	7	7	29	23	3	10
	napA	11	14	13	8	7	9	12	13	5	11
	napB	1	2	1	2	1	1	3	2	0	0
(assimilatory)	*narB*, no *A*	1	1	2	1	0	0	2	2	0	0
	nasA, no *B*	53	55	55	19	17	17	61	49	9	35
Nitrite reduction	*nirB*	10	12	12	8	6	9	12	13	3	10
	nirD	13	12	13	6	5	6	12	13	4	8
	nirA	0	0	1	0	1	0	0	0	0	0
	nrfA	2	2	2	1	1	1	2	1	1	2
	nrfH	0	1	0	0	0	0	0	0	0	1
	nirS	10	8	9	1	1	0	10	5	1	5
	nirK	10	8	9	1	1	0	10	5	1	5
Nitric oxide reduction	*norB*	28	27	26	11	7	9	31	26	5	17
	norC	14	13	12	8	5	6	15	13	0	7
Nitrous oxide reduction	*nosZ*	24	23	23	7	6	7	27	24	4	11
Nitrogen fixation	*nifD*	13	10	12	4	3	5	13	11	2	4
	nifK	10	6	10	3	3	3	11	8	2	4
	nifH	9	6	8	2	2	3	10	8	1	3

Figure 10. Sulfur and nitrogen metabolism related genes from the annotated metagenomic "detection" data from each sample. Gene counts are sums of all subunits if named together. Genes classified to certain reduction/oxidation reaction may also perform other reactions but are only listed once. The colours highlight the gene amounts and start to change from grey to blue with the first detected gene and from blue to purple after 10 detected genes. No colour change after 30 detected genes.

Metal resistance	Genes	Zn Rod mill feed June	Zn Rod mill feed November	Cu Rod mill feed June	Cu Rod mill feed November	Cu Concentrate thickener O/F June	Cu Concentrate thickener O/F November	TAI water June	TAI water November	ETAM Out June	ETAM Out November
Co-Zn-Cd/ Co-Ni	*czcA/cnrA*	123	138	125	65	47	51	129	112	37	77
	czcB/cnrB	77	81	78	40	33	31	81	67	29	51
	czcC/cnrC	61	72	72	38	37	37	70	57	19	43
Pb-Ca-Zn-Hg	*zntA*	44	49	60	27	34	29	49	45	10	31
Copper	*copA*	98	113	107	39	40	39	109	95	25	72
	copB	77	82	79	42	32	39	84	82	23	51
	copR	45	53	44	24	21	22	49	46	15	37
	copS	46	49	51	22	27	24	51	48	9	31
	pcoB	15	16	15	8	9	9	16	17	2	10
Arsenical	*arsB*	41	43	48	16	26	19	46	40	10	29
	arsC	85	94	94	39	38	43	96	89	23	58
	asrH	13	17	12	5	6	6	15	16	5	15
	arsR family	131	137	153	66	73	66	141	140	24	81
Nickel	*nreB*	5	5	6	1	3	2	4	4	3	3
	ncrA	0	0	0	0	0	0	0	0	0	0
Mercury	*merA*	40	40	46	18	22	16	45	39	11	27
	merP	35	34	32	16	12	10	36	32	12	20
	merR family	135	145	147	62	68	62	146	133	39	96
	merT	40	43	41	18	15	12	42	39	15	33
	merC	11	9	11	6	7	5	12	9	5	9
Chromate	*chrA*	30	41	45	20	27	20	36	35	11	32
Antibiotic resistance											
Aminoglycosides	*aadA*	0	0	0	0	0	0	0	0	0	0
	aadK	0	0	1	0	1	0	0	0	0	0
	strB	2	2	2	2	0	0	3	2	0	2
β-lactams	*ampC*	3	4	6	3	3	2	5	4	0	4
	ampG	27	34	32	15	14	15	29	27	5	19
Macrolides	*macA*	16	24	18	6	8	6	16	18	3	15
Sulfonamides	*sul1/2*	0	0	0	0	0	0	0	0	0	0
Tetracyclines	*tetM*	0	0	0	0	1	0	0	0	0	0
	tetA	8	6	8	3	3	2	7	9	4	6
Methicillin	*mecI*	2	3	2	1	1	1	2	3	0	1

Figure 11. Heavy metal and antibiotic resistance-related genes from each sample from the annotated metagenomic "detection" data. The colors highlight the gene amounts and start to change from grey to blue with the first detected gene and from blue to purple after 20 detected genes. No color change after 50 detected genes.

3.5. Microbial and Chemical Relationships

The principal coordinate analysis (PCoA, Figure 12) of the bacterial communities (amplicon sequencing data) together with chemical parameters showed no trend in placements between June and November samples but there was separation between sampling times for most sampling points. There was also a separation between the copper and zinc plant samples as the copper plant sample points mostly fell on the right side of the plot towards higher copper and lead concentrations, whereas the zinc plant and water circuit samples fell on the left side of the plot with higher magnesium concentrations. The raw water Santa Clara November samples were clearly separated from the other samples, but the June samples were clustered tightly in the centre of the plot amid the process samples. Based on the microbial taxonomy, the Santa Clara June and November samples contained the same taxonomical groups as the other samples, but the relative abundances were different from the other samples. Chemical parameters that affected the microbial communities most significantly ($p < 0.001$) were dissolved copper concentration, sulfate and TDS. In

addition, the amount of dissolved magnesium, potassium, sodium, lead and calcium and total sulfur significantly ($p < 0.01$) affected the bacteria. Concentrations of dissolved copper, lead and calcium, mostly affected the copper plant samples and dissolved magnesium affected the zinc plant samples. The in situ measured parameters T and redox showed a significant ($p < 0.001$) effect on bacterial communities (Figure S4). However, as all the in situ parameters were measured from only a limited number of samples, the analyses covered only about half of the samples, and no clear connection with any specific sample type and measured parameters was indicated.

The PCoA (Figure 13) of the archaeal communities together with chemical parameters showed a clear difference between the two samplings. This was perceptible for both samplings contained high and low sequence count samples, although generally the sequence counts were low. The June samples fell mostly to the right of the plot towards high tetrathionate and total thiosalts concentrations, while the corresponding November samples fell to the left. The Paste Thickener Overflow and the Santa Clara June samples clustered to the centre right of the plot, whereas the corresponding November samples fell to the upper right corner of the plot. The chemical variables statistically most significantly ($p < 0.001$) affecting the archaeal communities were the concentrations of tetrathionates, total thiosalts and dissolved copper and lead, which all affected to the bottom right of the plot where especially June samples from the copper process were situated. In addition, TDS and sulfate and nitrate concentrations also had significant ($p < 0.01$) effects. The in situ measurements were available only from five archaeal samples and therefore statistical relevance was low.

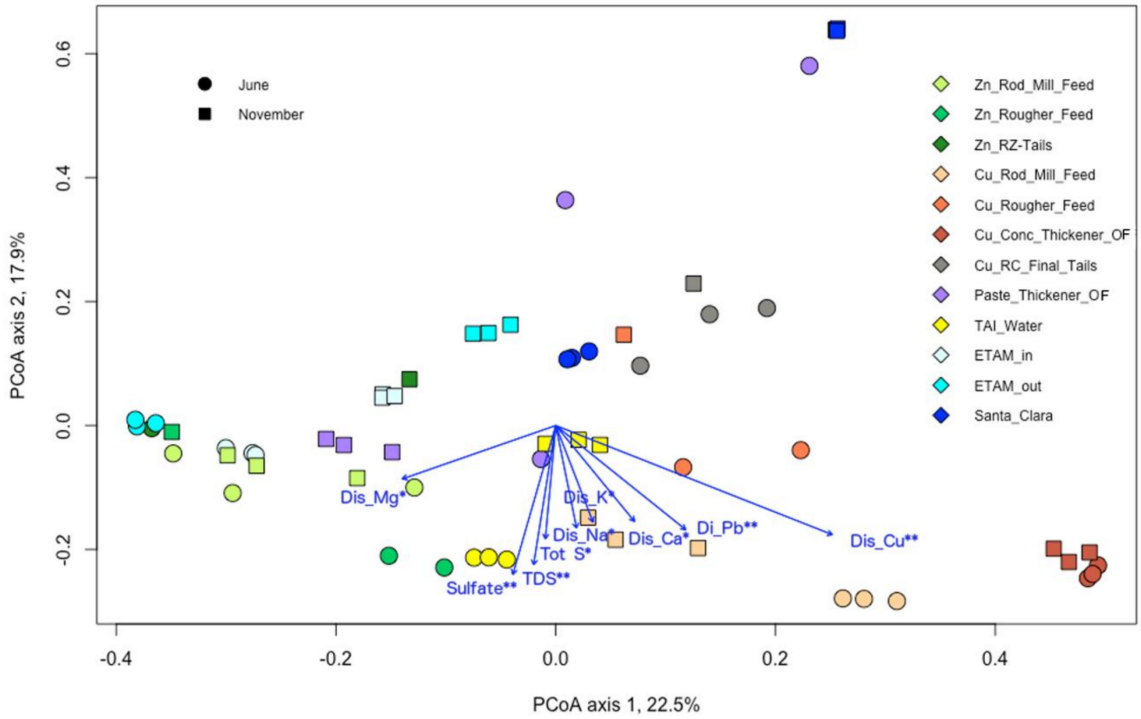

Figure 12. Principal coordinate analysis (PCoA) of the bacterial communities identified from the Portuguese mine zinc and copper plants and water circuit samples by the amplicon sequencing. Statistically significant (* $p < 0.01$, ** $p < 0.001$) chemical variables with 9999 permutations are indicated.

The PCoA (Figure 14) of the fungal communities together with chemical parameters did not show difference between the samplings. Dissolved copper had significant ($p < 0.001$) effect on the Cu Concentrate Thickener Overflow and the Cu Rod Mill Feed samples. Dissolved lead and potassium, tetrathionates and total thiosalts had also significant ($p < 0.001$)

effect on the fungal communities. In addition, in situ measured T significantly ($p < 0.001$) affected the Zn RZ Tails samples (Figure S5).

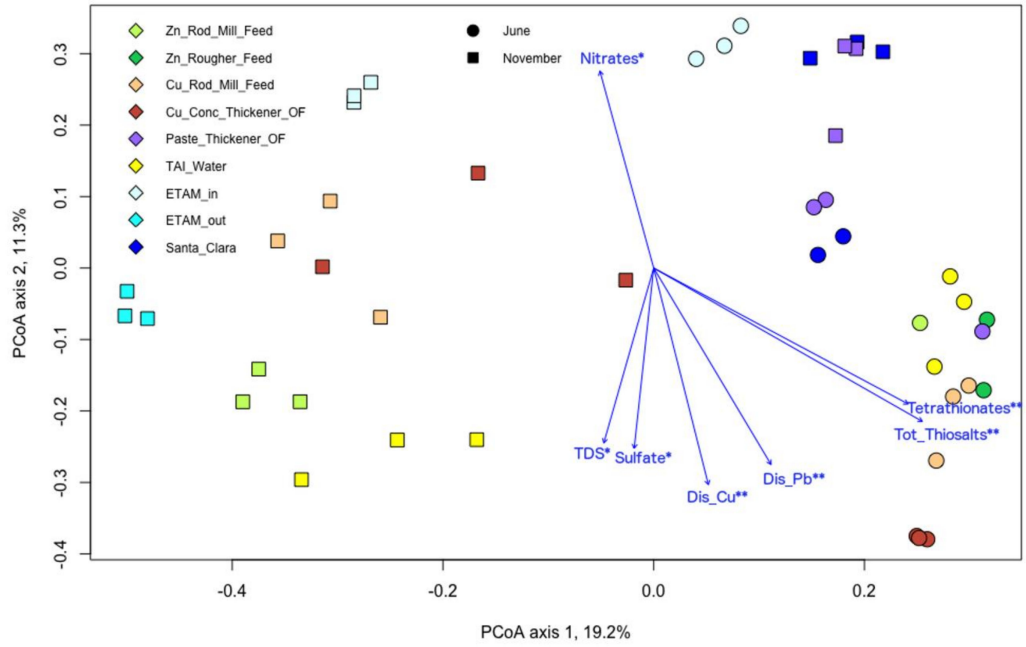

Figure 13. Principal coordinate analysis (PCoA) of the archaeal communities identified from the Portuguese zinc and copper plants and water circuit samples by amplicon sequencing. Statistically significant (* $p < 0.01$, ** $p < 0.001$) chemical variables with 9999 permutations are indicated.

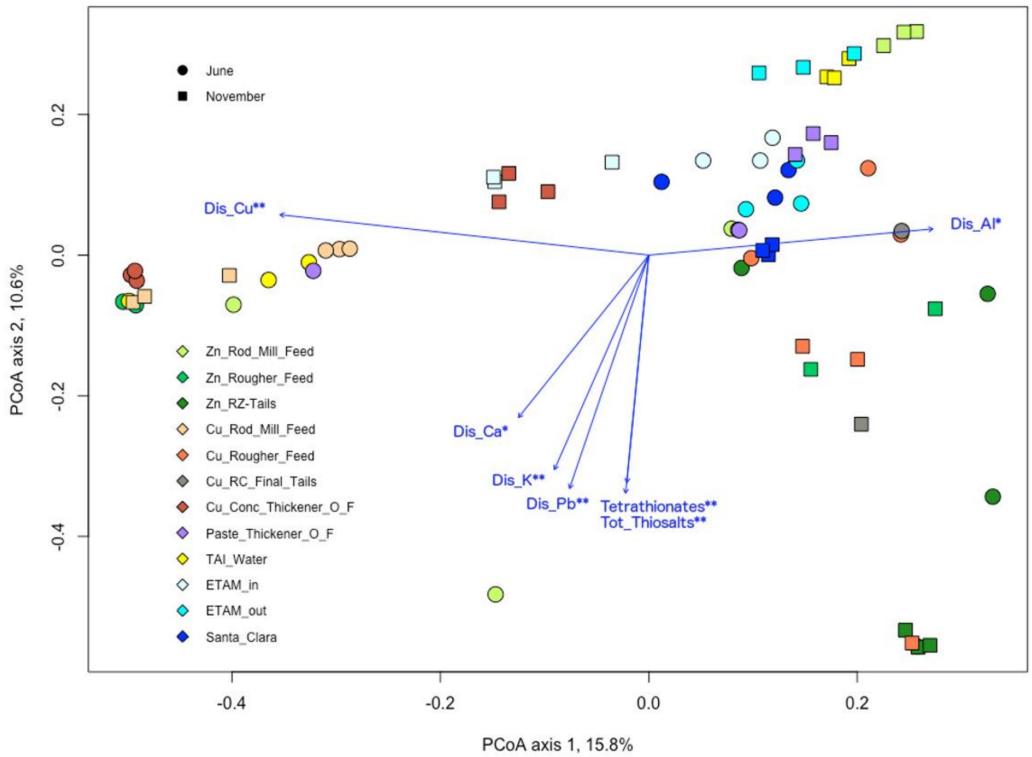

Figure 14. Principal coordinate analysis (PCoA) of the fungal communities identified from the Portuguese mine zinc and copper plants and water circuit samples by amplicon sequencing. Statistically significant (* $p < 0.01$, ** $p < 0.001$) chemical variables with 9999 permutations are indicated.

4. Discussion

In this study, we identified microbial communities present in abundance in different mineral processing steps combined with chemical data from the same points. Our results show that microorganisms are present in high numbers in different mineral processing steps. Bacteria dominated the microbial communities in the mine but in addition, both archaea and fungi were present in mineral processing environments. Overall, the bacteria detected in this Portuguese mine's zinc and copper processes and in the water circuit were highly selected to perform reduced sulfur compound oxidation based on knowledge of the detected 16S rRNA taxonomy and the metagenomic data. This was supported by the chemical data which showed that oxidative conditions existed in many parts of the process (Figure 2) also favouring chemical oxidation reactions. All samples were dominated with one, two or three sulfur oxidisers, i.e., *Thiovirga*, *Thiobacillus* and *Halothiobacillus*, but a multitude of other potentially sulfur metabolising groups, such as *Telmatospirillum*, *Alishewanella*, *Thermithiobacillus*, *Limnobacter,* Rhodobacteriacea and *Thiomonas* were present [48–55].

Thiovirga and *Thiobacillus*, the two most dominant genera are chemoautotrophic using sulfur compounds as electron donor and energy source and oxygen as electron acceptor. *Thiovirga sulfuroxydans,* is at present the only species in its genus and is able to oxidise elemental sulfur, sulfide and thiosulfate with an optimum pH and temperature at 7.5 and 30 °C, respectively [55]. However, the MAG that contained almost all 16S rRNA gene sequences identified as *Thiovirga*, had only genes for sulfide and thiosulfate (sox, fcc, and sqr) oxidation and not for elemental sulfur oxidation, which indicates that it may be a novel unidentified species of *Thiovirga* or another sulfur oxidiser. The *Thiobacillus* genus includes several species with varying metabolism but generally the species gain energy by oxidising reduced sulfur compounds, such as sulfides, sulfur, thiosulfate, polythionates, thiocyanate and in most cases also by oxidation of elemental sulfur [56]. *Thiobacillus thioparus* has a partial sox operon that contains *soxXYZAB* genes but is lacking *soxCD* [57], which is in accordance with our results showing less *soxCD* genes detected than other sox components in the sample communities (Figure 10). In the two *Thiobacillus* MAGs detected both complete and partial sox operons were found together with many sulfur/sulfate/sulfite/sulfide oxidation–reduction genes (*hdrB2*, *ETHE1*, *dsrAB*, *aprAB*, *sat*, *soeABC*, *sqr*). The *Thiobacillus* MAG with its partial sox complex, contained also genes for thiocyanate oxidation (*scnABC*) and tetrathionate and thiosulfate reduction (*ttrABC, phsAC*) demonstrating the variety of sulfur metabolism potential of this genus. *Thiobacillus* spp. have a pH optimum between 6 and 8 and a temperature range from 25 °C to 30 °C and up to 50 °C for *Thiobacillus aquaesulis* [56] features suitable for the studied processes. *Halothiobacillus* spp., which also oxidise reduced sulfur species for energy production and are regarded as halotolerant, were found in all samples and was especially common in the copper plant samples. *H. neapolitanus* has a pH optimum of 6.5–6.9 and a temperature optimum of 28–32 °C and a growth range from pH 4.5 to 8.5 and from 8 to 39 °C [58]. The *H. neapolitanus* MAG contained a partial sox complex (*soxZABCD*) and sulfide and thiosulfate oxidation genes (*sqr*, *ffcAB*, *tsdA*). However, the MAG was only 71.8% complete so some features may be lacking. Cu RC Final Tails offered conditions where another sulfur oxidiser, *Thermithiobacillus* was found more abundantly than other sulfur oxidizers. This genus includes two described species of which the first one is able to oxidise lead sulfide, thiosulfate and tetrathionate [59] and the other one a thermophilic sulfur oxidiser [60]. *Thiovirga* and *Halothiobacillus* have been detected from Kevitsa metal processing plant samples [10] but not as abundantly as from this Portuguese mine's process samples that were clearly more dominated by sulfur oxidation metabolism. This is likely related to the ores used in these plants as in Kevitsa mine sulfide minerals account for less than 5% of the total mineralogy [61] whereas the Iberian Pyrite is classified as a volcano-sedimentary massive sulfide. Several circum-neutral mine tailing reservoir waters in Canada were dominated either by Sphingomonadaceae and Rhodobactereaceae together with Burkholderiaceae or Halothiobacillaceae [62]. All of these were frequently detected also in the Portuguese mine's samples and in Kevitsa mine, indicating their adaptation to mineral processing waters. *Halothiobacillus* spp. were

an apparent part of the community in all the Portuguese mine's samples but *Thiovirga* dominated mostly in the zinc plant and water circuit samples and *Thiobacillus* more in the copper plant samples. This division between copper and zinc plant samples was visible also in the PCoA of the bacterial communities (Figure 12). Generally, the temperature and pH offered favourable conditions for the growth and activity of various sulfur oxidisers throughout the processes.

Even though potential for versatile sulfur metabolisms was detected by shotgun metagenomic analysis in the mineral processing plant microbial communities, we cannot conclude from this data how actively different sulfur compound pathways were transcribed and used in practice. Sulfur oxidizing groups were dominating in the 16S rRNA gene sequencing results and plenty of different reduced sulfur compounds were present in different process waters which could support the activity of sulfur oxidizing groups. Nevertheless, sulfide and thiosulfate oxidation-related genes (*sqr* and *sox*-complex) were numerically the most abundant sulfur oxidation–reduction genes indicating microorganisms possessing those genes to thrive in the mine mineral processing environments. In addition, nitrogen metabolism-related genes for especially nitrate and nitrite reduction/oxidation were abundant in addition to assimilative nitrate reduction genes. ATP synthesized during reduced inorganic sulfur oxidation can be produced by substrate-level phosphorylation or together with oxidative phosphorylation [63–65]. The ratio of detected S-compound and sulfide oxidation genes compared to detected oxidative phosphorylation and glycolysis genes was around 1:2. This indicates that also a high share of the microorganisms in the Portuguese mine belonged to clades that were not related to sulfur energy metabolism.

Most of the microorganisms detected in the Portuguese mineral processing plant are not known especially for iron oxidation ability. However, some minor groups, such as *Ferritrophicum* in TAI Water and *Ralstonia* in Cu Rougher Feed samples, are likely to perform aerobic iron oxidation [51,66]. *Ferritrophicum* and *Ralstonia* were found also in the Kevitsa mine process samples continuously during a two-month sampling period [10]. Flotation chemicals offer another source of carbon, nitrogen and phosphorus in the process and several bacteria are known to degrade xanthate used as a collector in flotation [67–69]. Many genera, such as *Acinetobacter*, *Pseudomonas*, *Diaphorobacter*, *Algoriphagus*, *Thauera*, *Sphingomonadaceae* and *Paraburkholderia*, which were detected in the samples, are able to perform aromatic compound and/or hydrocarbon degradation [70–76] and potentially participate in flotation chemical degradation.

Heavy metal resistance genes were abundantly detected in all studied process samples. Most of the studied heavy metal resistance genes were found from sulfur oxidising *Thiovirga*, *Thiobacillus* and *Halothiobacillus* MAGs and many with multiple copies. Other core microbiome members identified (at least 1% relative abundance in at least half of the samples) included *Pseudomonas* and *Diaphorobacter* OTUs. From the gained *Diaphorobacter* MAG (Figure S3), most of the studied heavy metal resistance genes were also identified and had the ability to reduce tetrathionate (*ttrABC*) and do denitrification and dissimilative nitrate reduction (*narGHI*, *nirBDS*, *norBC*, *nosZ*). This emphasizes that these core microorganisms have adapted to these extreme conditions and have advantages compared to microorganisms freshly entering the process.

There were many archaeal and fungal groups that were present with high relative abundance but identified only as unclassified archaea or unclassified fungi. It is possible that at least some of these uncultivated groups are specifically adapted to the mining environment, resistant to high metal concentrations and able to utilize the energy sources available. Some of those identified to the genus or class level and previously also found in mineral environments include for example, uncultured Thermoplasmatota group BSLdp215 that was found especially from ETAM Water and *Ferroplasma* from the Zn Rougher Feed. The group BSLdp215 has been found earlier in acidic iron-rich water from depths of 500 and 600 m from the Pyhäsalmi mine in Finland [77] and in deep, hot, basaltic rocks in India [78]; however, its role is unknown. *Ferroplasma*, on the other hand, are mesophilic, acidophilic and able to oxidize iron, pyrite and other metal sulfides; and they are often

found in acid mine drainage environments and ore deposits and mines [79]. Archaea may have a role in nitrogen cycling in this Portuguese mine, as ammonia oxidizing archaea from the Nitrosophaeria class were frequently detected. Fungal genera *Spencerozyma*, *Rhodotorula*, *Trichoderma* and *Talaromyces* that contain acid-tolerant and/or heavy metal tolerant (Cd, Pb, Ni, As) species [80–83] were found from the process water (TAI) which indicates that there are niches in the mineral processing plant that support fungal growth and their participation in the exploitation of the available nutrients. Interestingly, Malassezia were detected, especially in the zinc and copper Tails samples. Malassezia are generally recognized as a dominant part of the human skin's mycobiota [84], so they may have been found as a result of human contamination in these samples. However, Malassezia are also found from diverse environmental sources, such as deep-sea sediments [85], hydrothermal vents [86], Antarctic soils [87] and also recently from flotation tails of the Kevitsa mine in Finland [10].

It appears that the raw water from the Santa Clara reservoir had some role as a source of microorganisms for the process. The predominant microbial groups in the Santa Clara water both in June and November were not common in the process samples, except for the Paste Thickener Overflow microbiomes. The Santa Clara water mostly contained the bacterial groups Sporichthyaceae, CL-500-29_marine_group, SAR11, *Alishewanella*, *Thiovirga* and *Pseudomonas*. Nevertheless, all the dominant microbial groups of the process samples were detected in the raw water too, although not prominently. This connection was somewhat surprising as the conditions in the process are quite different from the raw water source. However, it is likely that these shared microbial groups were mostly only passing through the process. Escudero et al. [88] found that there are active bacterial and archaeal biofilms in the Iberian Pyrite Belt subsurface rocks at different depths at least until 519 m below the surface, indicating ore as one likely source of microorganisms in mineral processing.

The differences found in the process samples were relatively small in terms of bacterial, archaeal and fungal taxa between the two seasons. Temperatures measured in June and November samplings differed only 2 to 5 °C, depending on the sample point, weakening the expected temperature effect on microbial community composition. For this reason, it is likely that only one sampling time per season was not adequate to observe true seasonal changes, but other season independent variables affected more the microbial communities. Clear difference between samplings was visible only in the case of archaea (Figure 13) even though the overall sequence counts were relatively low for archaeal samples. There was no obvious reason visible in the PCoA with the measured chemical parameters included, even though chemical differences existed. The concentration of sulfate was higher in June than in November in all studied samples except for the Santa Clara water. Sulfate is generally the final product of the oxidation of sulfide [89], and as such an indication that the chemical oxidation activity was higher in June compared to November. The highest concentrations of thiosalts were found from the Zn Rougher Feed, the Cu RC Final Tails and the Paste Thickener Overflow samples. The peak in the concentration of thiosalts in the zinc plant was detected during the milling whereas the peak of thiosalts in the Cu plant was observed during the flotation. There are several possible explanations for this observation. It seems possible that the sulfidic minerals entering the Zn plant oxidize faster than the minerals used in the Cu plant. Additionally, since pH is a major factor that affects the oxidation of thiosalts [90], the kinetics of oxidations and the speciation of thiosalts likely differs between the two plants. This hypothesis is supported by the tetrathionate concentrations, which were almost twofold in the Zn plant than in the Cu plant. Thiosalts concentration and particularly its speciation can impact the flotation of sulfide ore due to its capacity to acidify the media and to reduce the ORP value [91,92]. Higher total thiosalt and tetrathionate concentrations in June may have had some effect on the archaeal diversity (Figure 13).

There was a difference in bacterial and archaeal communities of the raw water from Santa Clara between the samplings. In June the Santa Clara samples were more similar to the process samples but differentiated from most of the samples in November in the PCoAs

of bacteria and archaea (Figures 12 and 13). There were changes between the two samplings and sample points based on the metagenomic analysis (Figure 10 and Figure S2). However, no reasons for these differences were discovered from chemical or microbial data. Similar bacterial 16S rRNA gene copy counts and mapped read counts resulted for samples with high or low numbers of "detected" genes related to energy metabolism.

Other chemical observations potentially inhibiting or favouring different microbial groups include the concentration of magnesium, which was lower in the Cu plant than in the Zn plant. A possible explanation for the lower magnesium level may be the pH level in the Cu plant, which may precipitate magnesium [93]. Even though the concentrations of phosphorus and nitrogen were low, they were not limiting microbial growth and activity. The few elevated organic carbon and phosphorus concentrations detected were likely a consequence of additions of flotation and thickening reagents. In mineral processing, the majority of the nitrate originates from the explosives used in the pit. The residual nitrate from the ore can dissolve in the process water during grinding. Additionally, in the mine water treatment plant (ETAM) water from the pit is treated, which results in higher concentrations of nitrate in ETAM In and Out waters.

The microbiological procedures and methods provided good quality data but not from all the samples, as the extracted DNA amounts were too low (<0.05 ng/sample) for further analyses in some samples. The commercial DNA extraction kit functioned well for most mineral processing samples without modifications. However, the extraction of DNA was challenging for four sample points in both samplings, regardless of the fact that microorganisms were observed abundantly in these samples based on microscopy (Figure 6). This raises also the question of whether all different microorganism types have been equally detected from the rest of the samples or some part of the microbial population was so strongly attached to mineral particles that their DNA was not detached and thus not collected during the DNA extraction phase. In addition to the microbial communities detected in this study, there are likely other microorganisms present and possibly also with high abundance. These results clearly show that the DNA extraction methodologies for high mineral content samples need to be specifically developed.

5. Conclusions

Bacterial numbers in both copper and zinc flotation processes were high, but did not clearly reflect seasonal variation. Temperature, pH, phosphorus, nitrogen and carbon levels were suitable to support the growth and activity of various mesophilic microorganisms. Sulfur oxidisers were the prominent microbial group. Some of the microorganisms were well adapted to the flotation environments, demonstrated, for example, by the presence of heavy metal resistance genes in the core microorganisms, whereas some seemed only to merely pass through the process. Even though the microorganisms differed between the zinc and copper flotation plants due to the variable physico-chemical process parameters, the functions were similar, including sulfur, nitrogen and carbon metabolism. Since the microorganisms are present in high quantities in flotation; participate in the important chemical reaction processes, such as sulfur oxidation; and are also charged particles, their impacts on the flotation performance should be further evaluated.

Supplementary Materials: The following are available online at https://www.mdpi.com/2075-163X/11/2/156/s1. Procedure S1: Detailed analysis of the metagenomic sequence data. Figure S1: Bacterial phyla containing at a minimum 0.5% relative abundance in at least one sample. Figure S2: Energy metabolism-related genes from the annotated metagenomic "detection" data. Figure S3: Metagenome-assembled genomes (MAGs) manually binned in anvi'o showing over 70% completeness. Figure S4: Principal coordinate analysis of the bacterial communities identified from the Portuguese mine zinc and copper plants and water circuit samples by amplicon sequencing with chemical in situ variables. Figure S5 Principal coordinate analysis of the fungal communities identified from the Portuguese mine zinc and copper plants and water circuit samples by amplicon sequencing with chemical in situ variables. Table S1: Preservation and chemical analysis methods for water samples. Table S2: Average number of identified sequence reads, identified OTUs, estimated OTU richness and Shannon

diversity index calculated for the bacterial, archaeal and fungal triplicate samples. Table S3: Numbers of original and trimmed sequence reads and percentages of trimmed sequence reads mapping back to the co-assembly. Table S4: Information on the co-assembly. References [94,95] are cited in the supplementary materials.

Author Contributions: Conceptualization, H.M., M.B. and P.K.; methodology, H.M., M.B. and T.M.K.L.; software, M.B.; formal analysis, H.M., M.B. and T.M.K.L.; investigation, H.M. and T.M.K.L.; data curation, H.M., M.B. and T.M.K.L.; writing—original draft preparation, H.M., M.B. and T.M.K.L.; writing—review and editing, H.M., M.B., T.M.K.L., and P.K.; visualization, H.M., and T.M.K.L.; supervision, P.K.; project administration, P.K.; funding acquisition, P.K. All authors have read and agreed to the published version of the manuscript.

Funding: This project has received funding from the European Union's Horizon 2020 Research and Innovation program under grant Agreement number 730480, ITERAMS project (Integrated mineral technologies for more sustainable raw material supply).

Data Availability Statement: The bacterial, archaeal and fungal amplicon sequences and the metagenomic sequences have been submitted to the European Nucleotide Archive (http://www.ebi.ac.uk/ena) under study accession numbers PRJEB41552 and PRJEB42463, respectively.

Acknowledgments: Tuula Kuurila and Mirva Pyrhönen are thanked for invaluable assistance in the laboratory. The French Geological Survey (BRGM) is thanked for providing the raw in situ physicochemical data.

Conflicts of Interest: The authors declare no conflict of interest. The funders had no role in the design of the study, in the collection, analyses, or interpretation of data; in the writing of the manuscript, or in the decision to publish the results.

References

1. Johnson, D.B. The evolution, current status, and future prospects of using biotechnologies in the mineral extraction and metal recovery sectors. *Minerals* **2018**, *8*, 343. [CrossRef]
2. Liu, W.; Moran, C.J.; Vink, S. A reviw of the effect of water quality on flotation. *Miner. Eng.* **2013**, *53*, 91–100. [CrossRef]
3. Seifelnassr, A.A.S.; Abouzeid, A.-Z.M. Exploitation of bacterial activities in mineral industry and environmental preservation: An overview. *J. Min.* **2013**. [CrossRef]
4. Behera, S.K.; Mulaba-Bafubiandi, A.F. Microbes assisted mineral flotation a future prospective for mineral processing industries: A review. *Min. Proc Ext. Met. Rev.* **2017**, *38*, 96–105. [CrossRef]
5. Kinnunen, P.; Miettinen, H.; Bomberg, M. Review of potential microbial effects on flotation. *Minerals* **2020**, *10*, 533. [CrossRef]
6. Liu, W.; Moran, C.J.; Vink, S. Impact of chalcopyrite depression by water-borne bacteria in pure and combined mineral systems. *Int. J. Miner. Process.* **2013**, *123*, 18–24. [CrossRef]
7. Evdokimova, G.A.; Gershenkop, A.S.; Fokina, N.V. The impact of bacteria of circulating water on apatite-nepheline ore flotation. *J. Environ. Sci. Health Part A* **2012**, *47*, 398–404. [CrossRef]
8. Flemming, H.; Wuertz, S. Bacteria and archaea on Earth and their abundance in biofilms. *Nat. Rev. Microbiol.* **2019**, *17*, 247–260. [CrossRef]
9. Rampelotto, P.H. Extremophiles and extreme environments. *Life* **2013**, *3*, 482–485. [CrossRef]
10. Bomberg, M.; Miettinen, H.; Musuku, B.; Kinnunen, P. First insights to the microbial communities in the plant process water of the multi-metal Kevitsa mine. *Res. Microbiol.* **2020**, *171*, 230–242. [CrossRef]
11. Levay, G.; Smart, R.S.C.; Skinner, W.M. The impact of water quality on flotation performance. *J. S. Afr. Inst. Min. Metal.* **2001**, *101*, 69–76.
12. Muzinda, I.; Schreithofer, N. Water quality effects on flotation: Impacts and control of residual xanthates. *Miner. Eng.* **2018**, *125*, 34–41. [CrossRef]
13. Jucker, B.B.; Harms, H.; Zehnder, A.J.B. Adhesion of the positively charged bacterium *Stenotrophomonas* (*Xanthomonas*) *maltophilia* 70401 to glass and Teflon. *J. Bacteriol.* **1996**, *178*, 5472–5479. [CrossRef] [PubMed]
14. Stewart, E.J. Growing unculturable bacteria. *J. Bacteriol.* **2012**, *194*, 4151–4160. [CrossRef] [PubMed]
15. Le, T.M.K.; Miettinen, H.; Bomberg, M.; Schreithofer, N.; Dahl, O. Challenges in the assessment of mining process water quality. *Minerals* **2020**, *10*, 940. [CrossRef]
16. Herlemann, D.P.R.; Labrenz, M.; Jürgens, K.; Bertilsson, S.; Waniek, J.J.; Andersson, A.F. Transitions in bacterial communities along the 2000 km salinity gradient of the Baltic Sea. *ISME J.* **2011**, *5*, 1571–1579. [CrossRef]
17. Bano, N.; Ruffin, S.; Ransom, B.; Hollibaugh, J.T. Phylogenetic composition of Arctic Ocean archaeal assemblages and comparison with antarctic assemblages. *Appl. Environ. Microbiol.* **2004**, *70*, 781–789. [CrossRef]
18. Barns, S.M.; Fundyga, R.E.; Jeffries, M.W.; Pace, N.R. Remarkable archaeal diversity detected in a Yellowstone National Park hot spring environment. *Proc. Natl. Acad. Sci. USA* **1994**, *91*, 1609–1613. [CrossRef]

19. Bomberg, M.; Miettinen, H. Data on the optimization of an archaea-specific probe-based qPCR assay. *Data Brief* **2020**, *33*, 106610. [CrossRef]
20. Takai, K.E.; Horikoshi, K. Rapid detection and quantification of members of the archaeal community by quantitative PCR using fluorogenic probes. *Appl. Environ. Microbiol.* **2000**, *66*, 5066–5072. [CrossRef]
21. Haugland, R.; Vesper, S. Method of Identifying and Quantifying Specific Fungi and Bacteria. U.S. Patent Application No. 6,387,652, 14 May 2002.
22. Klindworth, A.; Pruesse, E.; Schweer, T.; Peplies, J.; Quast, C.; Horn, M.; Glöckner, F.O. Evaluation of general 16S ribosomal RNA gene PCR primers for classical and next-generation sequencing-based diversity studies. *Nucleic Acids Res.* **2013**, *41*, e1. [CrossRef] [PubMed]
23. Gardes, M.; Bruns, T.D. ITS primers with enhanced specificity for basidiomycetes—Application to the identification of mycorrhizae and rusts. *Mol. Ecol.* **1993**, *2*, 113–118. [CrossRef] [PubMed]
24. White, T.J.; Bruns, T.; Lee, S.; Taylor, J. Amplification and direct sequencing of fungal ribosomal RNA genes for phylogenetics. In *PCR Protocols: A Guide to Methods and Applications*; Innis, M.A., Gelfand, D.H., Sninsky, J.J., White, T.J., Eds.; Academic Press: New York, NY, USA, 1990; pp. 315–322.
25. Schloss, P.D.; Westcott, S.L.; Ryabin, T.; Hall, J.R.; Hartmann, M.; Hollister, E.B.; Lesniewski, R.A.; Oakley, B.B.; Parks, D.H.; Robinson, C.J.; et al. Introducing mothur: Open-source, platform-independent, community-supported software for describing and comparing microbial communities. *Appl. Environ. Microbiol.* **2009**, *75*, 7537–7541. [CrossRef] [PubMed]
26. Pruesse, E.; Quast, C.; Knittel, K.; Fuchs, B.M.; Ludwig, W.; Peplies, J.; Glöckner, F.O. SILVA: A comprehensive online resource for quality checked and aligned ribosomal RNA sequence data compatible with ARB. *Nucleic Acids Res.* **2007**, *35*, 7188–7196. [CrossRef]
27. Quast, C.; Pruesse, E.; Yilmaz, P.; Gerken, J.; Schweer, T.; Yarza, P.; Peplies, J.; Glöckner, F.O. The SILVA ribosomal RNA gene database project: Improved data processing and web-based tools. *Nucleic Acids Res.* **2013**, *41*, D590–D596. [CrossRef]
28. Altschul, S.F.; Gish, W.; Miller, W.; Myers, E.W.; Lipman, D.J. Basic local alignment search tool. *J. Mol. Biol.* **1990**, *215*, 403–410. [CrossRef]
29. Kõljalg, U.; Nilsson, R.H.; Abarenkov, K.; Tedersoo, L.; Taylor, A.F.S.; Bahram, M.; Bates, S.T.; Bruns, T.D.; Bengtsson-Palme, J.; Callaghan, T.M.; et al. Towards a unified paradigm for sequence-based identification of fungi. *Mol. Ecol.* **2013**, *22*, 5271–5277. [CrossRef]
30. Nilsson, R.H.; Larsson, K.H.; Taylor, A.F.S.; Bengtsson-Palme, J.; Jeppesen, T.S.; Schigel, D.; Kennedy, P.; Picard, K.; Glöckner, F.O.; Tedersoo, L.; et al. UNITE database for molecular identification of fungi: Handling dark taxa and parallel taxonomic classifications. *Nucleic Acids Res.* **2019**, *47*, D259–D264. [CrossRef]
31. UNITE Community. *UNITE Mothur Release*; UNITE Community: London, UK, 2017.
32. Caporaso, J.G.; Kuczynski, J.; Stombaugh, J.; Bittinger, K.; Bushman, F.D.; Costello, E.K.; Fierer, N.; Peña, A.G.; Goodrich, J.K.; Gordon, J.E.; et al. QIIME allows analysis of high-throughput community sequencing data. *Nat. Methods* **2010**, *7*, 335–336. [CrossRef]
33. Kassambara, A. ggpubr: "ggplot2" Based Publication Ready Plots, Version 0.4.0; R Package. 2020. Available online: https://CRAN.R-project.org/package=ggpubr (accessed on 28 January 2021).
34. Andrews, S.; Krueger, F.; Segonds-Pichon, A.; Biggins, L.; Cruger, C.; Wingett, S.; Montgomery, J. *FastQC: A Quality Control Tool for High Throughput Sequence Data*; Babraham Institute: Cambridge, UK, 2011; Available online: https://www.bioinformatics.babraham.ac.uk/projects/fastqc/ (accessed on 28 January 2021).
35. jstjohn/SeqPrep. Available online: https://github.com/jstjohn/SeqPrep (accessed on 11 November 2020).
36. Bolger, A.M.; Lohse, M.; Usadel, B. Trimmomatic: A flexible trimmer for illumina sequence data. *Bioinformatics* **2014**, *30*, 2114–2120. [CrossRef]
37. Li, D.; Liu, C.M.; Luo, R.; Sadakane, K.; Lam, T.W. MEGAHIT: An ultra-fast single-node solution for large and complex metagenomics assembly via succinct de Bruijn graph. *Bioinformatics* **2015**, *31*, 1674–1676. [CrossRef] [PubMed]
38. Eren, A.M.; Esen, Ö.C.; Quince, C.; Vineis, J.H.; Morrison, H.G.; Sogin, M.L.; Delmont, T.O. Anvi'o: An advanced analysis and visualization platform for 'omics data. *PeerJ* **2015**, *3*, e1319. [CrossRef] [PubMed]
39. Langmead, B.; Salzberg, S.L. Fast gapped-read alignment with Bowtie 2. *Nat. Methods* **2012**, *9*, 357. [CrossRef] [PubMed]
40. Menzel, P.; Ng, K.L.; Krogh, A. Fast and sensitive taxonomic classification for metagenomics with Kaiju. *Nat. Commun.* **2016**, *7*, 1–9. [CrossRef] [PubMed]
41. El-Gebali, S.; Mistry, J.; Bateman, A.; Eddy, S.R.; Luciani, A.; Potter, S.C.; Qureshi, M.; Richardson, L.J.; Salazar, G.A.; Smart, A.; et al. The Pfam protein families database in 2019. *Nucleic Acids Res.* **2019**, *47*, D427–D432. [CrossRef]
42. Seemann, T. Prokka: Rapid prokaryotic genome annotation. *Bioinformatics* **2014**, *30*, 2068–2069. [CrossRef]
43. Kanehisa, M.; Sato, Y.; Kawashima, M.; Furumichi, M.; Tanabe, M. KEGG as a reference resource for gene and protein annotation. *Nucleic Acids Res.* **2016**, *44*, D457–D462. [CrossRef]
44. Parks, D.H.; Imelfort, M.; Skennerton, C.T.; Hugenholtz, P.; Tyson, G.W. CheckM: Assessing the quality of microbial genomes recovered from isolates, single cells, and metagenomes. *Genome Res.* **2015**, *25*, 1043–1055. [CrossRef]
45. Greet, C.J. Chapter 1: The Eureka mine—An example of how to identify and solve problems in a flotation plant. In *Flotation Plant Optimisation: A Metallurgical Guide to Identifying and Solving Problems in Flotation Plants*; Greet, C.J., Ed.; Australasian Institute of Mining and Metallurgy: Carlton South, NSW, Australia, 2010; pp. 1–33.

46. McMurdie, P.J.; Holmes, S. phyloseq: An R package for reproducible interactive analysis and praphics of microbiome census data. *PLoS ONE* **2013**, *8*, e61217. [CrossRef]
47. Oksanen, J.; Blanchet, G.F.; Friendly, M.; Kindt, R.; Legendre, P.; McGlinn, D.; Minchin, P.R.; O'Hara, R.B.; Simpson, G.L.; Solymos, P.; et al. Vegan: Community Ecology Package, Version 2.5-6; R Package. 2009. Available online: https://CRAN.R-project.org/package=vegan (accessed on 28 January 2021).
48. Hammer, Ø.; Harper, D.A.; Ryan, P.D. PAST: Paleontological statistics software package for education and data analysis. *Palaeontol. Electron.* **2001**, *4*, 9.
49. Hausmann, B.; Pjevac, P.; Schreck, K.; Gerbold, C.W.; Daims, H.; Wagner, M.; Loy, A. Draft genome sequence of Telmatospirillum siberiense 26-4b1, an acidotolereant peatland alphaproteobacterium potentially involved in sulfur cycling. *Genome Announc.* **2018**, *6*, e01524-17. [CrossRef] [PubMed]
50. Xia, X.; Li, J.; Liao, S.; Zhou, G.; Wang, H.; Li, L.; Xu, B.; Wang, G. Draft genomic sequence of a chromate- and sulfate-reducing Alishewanella strain with the aility ro bioremediate Cr and Cd contamination. *Stand. Genomic Sci.* **2016**, *11*, 48. [CrossRef] [PubMed]
51. Watanabe, T.; Miura, A.; Shinohara, A.; Kojima, H.; Fukui, M. Thermithiobacillus plumbiphilus sp. nov., a sulfur-oxidizing bacterium isolated from lead sulfide. *Int. J. Syst. Evol. Microbiol.* **2016**, *66*, 1986–1989. [CrossRef] [PubMed]
52. Lee, C.S.; Kim, K.K.; Aslam, Z.; Lee, S.-T. Rhodanobacgter thiooxydans sp. nov., isolated from a biofilm on sulfur particles used in an autotrophic denitrification process. *Int. J. Syst. Evol. Microbiol.* **2007**, *57*, 1775–1779. [CrossRef]
53. Spring, S.; Kämpfer, P.; Schleifer, K.H. Limnobacter thiooxidans gen. nov., sp. novel thiosulfate-oxidazing bacterium isolated from freshwater lake sediment. *Int. J. Syst. Evol. Microbiol.* **2001**, *51*, 1463–1470. [CrossRef]
54. Chen, X.-G.; Geng, A.-L.; Gould, W.D.; Ng, Y.-L.; Liang, D.T. Isolation and characterization of sulphur-oxidizing *Thiomonas* sp. and its potential application in biological deodorization. *Lett. Appl. Microbiol.* **2004**, *39*, 495–503. [CrossRef]
55. Ito, T.; Sugita, K.; Yumoto, I.; Nodasaka, Y.; Okabe, S. *Thiovirga* sulfuroxydans gen. nov., sp. nov., a chemolithoautotrophic sulfur-oxidizing bacterium isolated from a microaerobic waste-water biofilm. *Int. J. Syst. Evol. Microbiol.* **2005**, *55*, 1059–1064. [CrossRef]
56. Robertson, L.A.; Kuenen, J.G. The genus Thiobacillus. In *Prokaryotes, Proteobacteria: Alpha and Beta Subclasses*; Dworkin, M., Falkow, S., Rodenberg, E., Schleifer, K.-H., Stackebrandt, E., Eds.; Springer: New York, NY, USA, 2006; Volume 5, pp. 812–827.
57. Hutt, L.P.; Huntemann, M.; Clum, A.; Pillay, M.; Palaniappan, K.; Varghese, N.; Mikhailova, N.; Stamatis, D.; Reddy, T.; Daum, C.; et al. Permanent draft genome of *Thiobacillus thioparus* DSM 505^{T}, an obligately chemolithoautotrophic member of the Betaproteobacteria. *Stand. Genomic Sci.* **2017**, *12*, 10. [CrossRef]
58. Kelly, D.P.; Wood, A.P.; Genus, I. Halothiobacillus. In *Bergey's Manual of Systematic Bacteriology*, 2nd ed.; Brenner, D.J., Krieg, N.R., Staley, J.T., Garrity, G.M., Eds.; Springer: New York, NY, USA, 2005; Volume 2.
59. Wood, A.P.; Kelly, D.P. Physiological characteristics of a new thermophilic obligately chemolithotrophic *Thiobacillus* species *Thiobacillus tepidarius*. *Int. J. Syst. Bacteriol.* **1985**, *35*, 434–437. [CrossRef]
60. Musuku, B.; Muzinda, I.; Lumsden, B. Cu-Ni processing improvements a First Quantum's Kevitsa mine. *Miner. Eng.* **2015**, *88*, 9–17. [CrossRef]
61. Whaley-Martin, K.; Jessen, G.L.; Colenbrander Nelson, T.; Mori, J.F.; Apte, S.; Jarolimek, C.; Warren, L.A. The potential role of *Halothiobacillus* spp. In sulfur oxidation and acid generation in circum-neutral mine tailings reservoirs. *Front. Microbiol.* **2019**, *10*, 297. [CrossRef] [PubMed]
62. Narayan, K.D.; Sabat, S.C. Mechanism of electron transport during thiosulfate oxidation in an obligately mixotrophic bacterium *Thiomonas bhubaneswarensis* strain S10 (DSM 18181^{T}). *Appl. Microbiol. Biotech.* **2017**, *101*, 1239–1252. [CrossRef] [PubMed]
63. Dopson, M.; Lindström, E.B.; Hallberg, K.B. ATP generation during reduced inorganic sulfur compound oxidation by *Acidithiobacillus caldus* is exclusively due to electron transport phosphorylation. *Extremophiles* **2002**, *6*, 123–129. [CrossRef] [PubMed]
64. Aminuddin, M. Substrate level versus oxidative phosphorylation in the generation of ATP in *Thiobacillus denitrificans*. *Arch. Micrbiol.* **1980**, *128*, 19–25. [CrossRef]
65. Weiss, J.V.; Rentz, J.A.; Olaia, T.; Neubauer, S.C.; Merrill-Floyd, M.; Lilburn, T.; Bradburne, C.; Megonigal, P.; Emerson, D. Characterization of neutrophilic Fe(II)-oxidizing bacteria isolated from the rhizosphere of wetland plants and description of *Ferritrophicum radicicola* gen. nov. sp. nov., and *Sideroxydans paludicola* sp. nov. *Geomicrobiol. J.* **2007**, *24*, 559–570. [CrossRef]
66. Swanner, E.D.; Nell, R.M.; Templeton, A.S. Ralstonia species mediate Fe-oxidation in circumneutral, metal-rich subsurface fluids of Henderson mine, CO. *Chem. Geol.* **2011**, *284*, 339–350. [CrossRef]
67. Natarajan, K.A.; Sabari Prakasan, M.R. Biodegradation of sodium isopropyl xanthate by *Paenibacillus polymyxa* and *Pseudomonas putida*. *Miner. Metall. Proc.* **2013**, *30*, 226–232. [CrossRef]
68. Chen, S.; Gong, W.; Mei, G. Study on biodegradation of alkyl xanthate collectors. In Proceedings of the 4th International Conference on Bioinformatics and Biomedical Engineering, Chengdu, China, 18–20 June 2010; pp. 1–6. [CrossRef]
69. Chen, S.; Li, S.; Xiong, P.; Du, D. Biodegradation of sodium butyl xanthate by *Shewanella oneidensis* MR-1 in the presence of Cr(VI). *Environ. Eng. Sci.* **2019**, *36*, 1179. [CrossRef]
70. Fewson, C.A. Metabolism of aromatic compounds by acinetobacter. In *The Biology of Acinetobacter. Federation of European Microbiological Societies Symposium Series*; Towner, K.J., Bergogne-Bérézin, E., Fewson, C.A., Eds.; Springer: Boston, MA, USA, 1991; Volume 57.

71. Jiménez, J.I.; Nogales, J.; García, J.L.; Díaz, E. A genomic view of the catabolism of aromatic compounds in pseudomonas. In *Handbook of Hydrocarbon and Lipid Microbiology*; Timmis, K.N., Ed.; Springer: Berlin/Heidelberg, Germany, 2010.
72. Wang, P.; Zhang, Y.; Jin, J.; Wang, T.; Wang, J.; Jiang, B. A high-efficiency phenanthrene-degrading *Diaphorobacter* sp. isolated from PAH-contaminated river sediment. *Sci. Total Environ.* **2020**, *746*, 140455. [CrossRef]
73. Wang, W.; Zhong, R.; Shan, D.; Shao, Z. Indigenous oil-degrading bacteria in crude oil-contaminated seawater of the Yellow sea, China. *Appl. Microbiol. Biotechnol.* **2014**, *98*, 7253–7269. [CrossRef]
74. Mao, Y.; Zhang, X.; Xia, X.; Zhong, H.; Chao, L. Versatile aromatic compound-degrading capacity and microdiversity of Thauera strains isolated from a coking wastewater treatment bioreactor. *J. Ind. Microbiol. Biotechnol.* **2010**, *37*, 927–934. [CrossRef] [PubMed]
75. Kertesz, M.A.; Kawasaki, A. Hydrocarbon-degrading Sphingomonads: Sphingomonas, Sphingobium, Novosphingobium, and Sphingopyxis. In *Handbook of Hydrocarbon and Lipid Microbiology*; Timmis, K.N., Ed.; Springer: Berlin/Heidelberg, Germany, 2010.
76. Morya, R.; Salvachúa, D.; Shekahar Thakur, I. Burkholderia: An untapped but promising bacterial genus for the conversion of aromatic compounds. *Trends Biotechnol.* **2020**, *38*, 963–975. [CrossRef] [PubMed]
77. Bomberg, M.; Mäkinen, J.; Salo, M.; Kinnunen, P. High diversity in iron cycling microbial communities in acidic, iron-rich water of the Pyhäsalmi mine, Finland. *Geofluids* **2019**. [CrossRef]
78. Dutta, A.; Sar, P.; Sarkar, J.; Dutta Gupta, S.; Gupta, A.; Bose, H.; Mukherjee, A.; Roy, S. Archaeal communities in deep terrestrial subsurface underneath the Deccan Traps, India. *Front. Microbiol.* **2019**, *10*, 1362. [CrossRef]
79. Golyshina, O.V.; Lünsdorf, H.; Golyshin, P.N. Ferroplasma. In *Bergey's Manual of Systematic of Archaea and Bacteria*; Whitman, W.B., Rainey, F., Kämpfer, P., Trujillo, M., Chun, J., DeVos, P., Hedlund, B., Dedysh, S., Eds.; John Wiley and Sons: Hoboken, NJ, USA, 2016.
80. Yang, B.-C.; Chen, N.; Liao, B.; Huang, Y.; Huang, L.-N. *Spencerozyma acididurans* sp. nov., an acid-tolerant basidiomycetous yeast species isolated from acid mine drainage. *Int. J. Syst. Evol. Micr.* **2019**, *69*, 2828–2833. [CrossRef]
81. Salinas, E.; Elorza de Orellano, M.; Rezza, I.; Martinex, L.; Marchesvky, E.; Sanz de Tosetti, M. Removal of cadmium and lead from dilute aqueous solutions by Rhodotorula rubra. *Bioresour. Technol.* **2000**, *72*, 107–112. [CrossRef]
82. Hoseinzadeh, S.; Shahabivand, S.; Aliloo, A.A. Toxic metals accumulation in *Trichoderma asperellum* and *T. harzianum*. *Microbiology* **2017**, *86*, 728–736. [CrossRef]
83. Nam, I.-H.; Murugesan, K.; Ryu, J.; Kim, J.H. Arsenic (As) removal using *Talaromyces* sp. KM-31 isolated from As-contaminated mine soil. *Minerals* **2019**, *9*, 568. [CrossRef]
84. Findley, K.; Oh, J.; Yang, J.; Conlan, S.; Deming, C.; Meyer, J.A.; Schoenfeldt, D.; Nomicos, E.; Park, M.; Kong, H.H.; et al. Topographic diversity of fungal and bacterial communities in human skin. *Nature* **2013**, *498*, 367–370. [CrossRef]
85. Lai, X.; Cao, L.; Tan, H.; Fang, S.; Huang, Y.; Zhou, S. Fungal communities from methane hydrate-bearing deep-sea marine sediments in South China Sea. *ISME J.* **2007**, *1*, 756–762. [CrossRef]
86. Le Calvez, T.; Burgaud, G.; Mahe, S.; Barbier, G.; Vandenkoornhuyse, P. Fungal diversity in deep-sea hydrothermal ecosystems. *Appl. Environ. Microbiol.* **2009**, *75*, 6415–6421. [CrossRef] [PubMed]
87. Arenz, B.E.; Held, B.W.; Jurgens, J.A.; Farrell, R.L.; Blanchette, R.A. Fungal diversity in soils and historic wood from the Ross Sea Region of Antarctica. *Soil Biol. Biochem.* **2006**, *38*, 3057–3064. [CrossRef]
88. Escudero, C.; Vera, M.; Oggerin, M.; Amils, R. Active microbial biofilms in deep poor porous continental subsurface rocks. *Sci. Rep.* **2017**, *8*, 1538. [CrossRef] [PubMed]
89. Vongporm, Y. Thiosalt Behaviour in Aqueous Media. Ph.D. Thesis, Memorial University of Newfoundland, Saint John, NL, Canada, 2008; pp. 26–36.
90. Miranda-Trevino, J.C.; Pappoe, M.; Hawboldt, K.; Bottaro, C. The importance of thiosalts speciation: Review of analytical methods, kinetics, and treatment. *Crit. Rev. Environ. Sci. Technol.* **2013**, *43*, 2013–2070. [CrossRef]
91. Liu, L.; Rao, S.R.; Finch, J.A. Technical note laboratory study of effect of recycle water on flotation of a Cu/Zn sulphide ore. *Miner. Eng.* **1993**, *6*, 1183–1190. [CrossRef]
92. Öztürk, Y.; Bıçak, Ö.; Özdemir, E.; Ekmekçi, Z. Mitigation negative effects of thiosulfate on flotation performance of a Cu-Pb-Zn sulfide ore. *Miner. Eng.* **2018**, *122*, 142–147. [CrossRef]
93. Phillips, V.A.; Kolbe, J.L.; Opperhauser, H. Effect of pH on the growth of $Mg(OH)_2$ crystals in an aqueous environment at 60 °C. *J. Cryst. Growth* **1977**, *41*, 228–234. [CrossRef]
94. Mikheenko, A.; Saveliev, V.; Gurevich, A. MetaQUAST: Evaluation of metagenome assemblies. *Bioinformatics* **2016**, *32*, 1088–1090. [CrossRef]
95. Ondov, B.D.; Bergman, N.H.; Phillippy, A.M. Krona: Interactive metagenomic visualization in a web browser. In *Encyclopedia of Metagenomics*; Springer US: New York, NY, USA, 2015; pp. 339–346.